Air–sea CO_2 exchange in the Southern Adriatic Sea: assessing its role as a moderate carbon sink over the last decade (2015-2024)

Carlotta Dentico[1,2],, Gianpiero Cossarini[2], Giuseppe Civitarese[2], Michele Giani[2], Angelo Rubino[1] and Vanessa Cardin[2]

[1] Department of Environmental Sciences, Informatics and Statistics, Università Cà Foscari, Venice, Italy
[2] National Institute of Oceanography and Applied Geophysics (OGS), Trieste, Italy

Correspondence to: Carlotta Dentico (cdentico@ogs.it)

Abstract

Coastal waters contribute significantly to the total oceanic carbon uptake. In this context, the cumulative influence exerted by marginal seas may be conspicuous. However sparse and unevenly distributed observations in such regions pose a serious limit to an accurate, experimentally based quantification of carbon dynamics. The Southern Adriatic (SAd) is one of the key sites of the Mediterranean Sea where open-ocean deep water formation occurs, a process recognized as a major driver of carbon sequestration. However, observations in this region remained sparse, thus ~~only a limited number of studies have investigated~~ quantitative assessment of surface carbon dynamics and ~~quantified~~ air-sea carbon flux are still limited ~~in the Sad~~. In this study, a ~~newly~~ recently validated, decade-long (2015-2024) high-resolution time series of surface partial pressure of CO_2 (pCO_{2sw})~~CO_2~~ and hydrographic measurements collected at the EMSO-E2M3A South Adriatic observatory, located at the center of the Southern Adriatic Pit, has been analysed. The results showed that seasonal temperature variability and winter vertical mixing were the dominant drivers of pCO_{2sw} variability, with biological processes likely contributing during the post-convective period. ~~seasonal temperature variability and winter convection were the main processes driving the dynamics~~ of ~~surface partial pressure of CO_2 (pCO_{2sw})~~. Air–sea CO_2 flux (FCO_2), derived from in situ observations, indicated a clear seasonal pattern, with the SAd acting as a CO_2 sink during winter and as a source during summer. Importantly, the results revealed that the SAd acted as a weak-to-moderate annual carbon sink over the last decade. However, the magnitude of FCO_2, was strongly influenced by the selected gas transfer velocity parametrization. Similalry, the use of a different wind speed input, for instance ERA5 reanalysis, also altered the estimated CO_2 flux, highlighting the importance of carefully selecting wind products for regional air-sea FCO_2 calculations. ~~Uncertainty analysis in the flux estimates were also evaluated, revealing that wind speed input data used for FCO_2 calculations influenced the magnitude of FCO_2~~. Finally, the results presented here showed how time series such as the SAd dataset can serve as critical assets for validating operational ocean

models, such as the ~~EU~~ European Copernicus Marine Service for the Mediterranean, by helping to identify discrepancies in the simulation of key processes.

1. Introduction

In the decade 2014-2023 it is estimated that the ocean has absorbed 10.5 $GtCO_2$ on average each year, which corresponds to around 26% of total carbon dioxide (CO_2)~~CO_2~~ emissions (Friedlingstein et al., 2025). The concentration of ~~carbon dioxide (~~CO_2~~)~~ in the atmosphere has increased from approximately 278 parts per million (ppm) at the beginning of the Industrial Revolution (Gulev et al., 2021), to more than 421 ppm at the end of 2024 (Lan et al., 2024). This has led to an increasing ocean carbon uptake, which, in turn, has caused changes in seawater chemistry (Doney et al., 2009; Gattuso and Hansson, 2011) negatively affecting many marine organisms and ecosystems (e.g., Ilyina et al., 2009; Lohbeck et al., 2012; Meyer and Riebesell, 2015). Air-sea CO_2 exchange is primarily controlled by the difference between the partial pressure of CO_2 in seawater and in the atmosphere, by the solubility of CO_2, and by the gas transfer velocity. While CO_2 solubility mainly depends on temperature and salinity and is relatively well constrained (Weiss, 1974), the gas transfer velocity is controlled by a complex set of physical processes, including molecular diffusion, turbulent mixing, surface waves, bubbles, and spray. It is parameterised as a function of wind speed, and several polynomial relationships have been fitted between the gas transfer velocity and the wind speed based on field experiments (e.g., Wanninkhof and McGillis, 1999; Nightingale et al., 2000). Because no consensus exists on the optimal gas transfer velocity parameterisation, the choice and quality of wind speed data can strongly influence air-sea CO_2 flux estimates (Wanninkhof, 1992; Naegler et al., 2006; Otero et al., 2013). In situ wind measurements are generally preferred when available (Otero et al., 2013), but they, as well air temperature, may not be measured at the same time and location of marine CO_2 and salinity observations, especially in buoy-based observing systems. Model- or satellite-derived winds are therefore often used as alternatives, although they also introduce additional sources of uncertainty (Otero et al., 2013).

~~The CO_2 absorbed by the ocean reacts with seawater to form carbonic acid (H_2CO_3), much of which dissociates releasing hydrogen ions (H^+), bicarbonate (HCO_3^-), and, to a lesser extent, carbonate ions (CO_3^{2-}) according to the salinity, pressure and temperature dependent equilibrium constants (Zeebe & Wolf-Gladrow, 2001). The increased concentration of hydrogen ions causes a reduction of pH and of carbonate ions in seawater. This process is commonly referred to as ocean acidification (Doney et al., 2009; Gattuso and Hansson, 2011) and is one of the major threats to many marine organisms~~. ~~Carbonate ions are an important building block of structures such as sea shells and coral skeletons. Decreases in carbonate ions can make building and maintaining shells and other calcium carbonate structures more difficult for calcifying organisms such as shellfish, corals and calcareous plankton (e.g., Ilyina et al., 2009; Lohbeck et al., 2012; Meyer and Riebesell, 2015) putting on risk the entire food web.~~

E~~Global e~~stimates of the global CO_2 air-sea flux ~~ocean carbon flux~~ therefore rely on both observations and models (Gruber et al., 2023; Fay et al., 2024; Friedlingstein et al., 2025). Many efforts have been made by the scientific community to increase the number and availability of carbon measurements from different sources (e.g., from research vessels, autonomous sensors, Argo floats) into quality controlled and openly accessible data products, resulting ~~in more than 30~~ in 44 million observations in the Surface Ocean CO_2 Atlas (SOCAT) V2026~~2~~ release (Bakker et al., 2026). However, these observations cover only a small fraction of the ocean surface and the amount of new observations per year in the open ocean has decreased since 2017 (Bakker et al., 2023). In situ observations are of paramount importance to provide high spatiotemporal resolution in specific areas of interest, to monitor Essential Ocean Variables (EOVs), to inform about ocean conditions throughout the water column (Tanhua et al., 2019; Schroeder et al., 2023) and to assess the quality of different model products and satellite measurements. Ocean reanalyses have demonstrated significant potential in bridging observational gaps by providing comprehensive, three-dimensional, basin-wide datasets that enable the investigation of spatial and temporal variability across multiple scales (Cossarini et al., 2021). However, generating a coupled physical-biogeochemical reanalysis remains a complex challenge (Park et al., 2018), due to uncertainties in the representation of interactions between physical and biogeochemical processes, the limited availability of biogeochemical observations for both data assimilation and validation, and the multivariate nature of the biogeochemical system, which involves intricate relationships between observed and modeled variables (Cossarini et al., 2021). As a result, models still struggle to accurately represent sparsely sampled regions, and considerable uncertainties persist, particularly in marginal and coastal seas (Resplandy et al., 2024). Despite their small size (about 7% of the global ocean area), marginal and coastal seas have a significant impact on the carbon cycle (Lee et al., 2011; Kapsenberg et al., 2017; Laruelle et al., 2018; Hassoun et al., 2019; Resplandy et al., 2024). ~~The latest~~ Recent estimates from Roobaert et al. (2024) quantified the global coastal CO_2 flux equal to -2.2 $GtCO_2$ yr^{-1} (-0.6 PgC yr^{-1}) which represent around 21% of the total current CO_2 flux from the atmosphere to the ocean (10.5 $GtCO_2$; Friedlingstein et al., 2025). The seawater carbonate system in these regions is driven by complex interaction between physical and chemical processes, like the overturning circulation, ocean mixing, freshwater inputs and biological processes. These interactions vary over time and space highlighting the importance of sustained time series observations to better understand and separate their individual contributions (Garcia-Ibañez et al., 2024). ~~Thus, in situ observations are of paramount importance to provide high spatiotemporal resolution in specific areas of interest, to monitor Essential Ocean Variables (EOVs), to inform about ocean conditions throughout the water column (Schroeder et al., 2022) and to assess the quality of different model products and satellite measurements.~~

The Mediterranean Sea is a semi-enclosed basin, where Atlantic Ocean water is exchanged through the Strait of Gibraltar ~~and is one of the areas where CO_2 estimations remain sparse and unevenly distributed (Hassoun et al., 2022)~~. Compared to the global ocean, it is characterized by a peculiar carbonate system. As a concentration basin, where evaporation exceeds precipitation, it is characterized by high salinity and elevated total alkalinity and dissolved inorganic carbon concentrations (Álvarez et al., 2023, 2026). Together with its active overturning circulation and the presence of several dense water formation regions, these characteristics promote an efficient uptake and transport of anthropogenic CO_2 to the ocean interior. In addition, a low Revelle factor, provides a high buffering capacity against increasing atmospheric CO_2 compared to other oceanic regions (Álvarez et al., 2014; Hassoun et al., 2019; Álvarez et al., 2023). Within the Mediterranean Sea, two major overturning circulation cells contribute to transporting carbon from the surface to the ocean interior (Lee et al., 2011). In the eastern Mediterranean, the northern and southern Adriatic play a key role in sustaining the thermohaline circulation (Robinson et al., 2001) and in capturing and storing CO_2 in the deeper layers (Cantoni et al., 2016; Ingrosso et al., 2017; Urbini et al., 2020; Cantoni et al., 2024). In particular, the Northern Adriatic Deep Water represents the densest and most CO_2-rich water mass in the region, significantly contributing to deep ventilation and carbon sequestration in the eastern Mediterranean basin. Despite the importance of the Mediterranean Sea for the regional carbon cycle, observational coverage remains sparse and unevenly distributed (Hassoun et al., 2022). According to the SOCAT V2026 (Bakker et al., 2026) there is a marked imbalance in data availability across Mediterranean regions, with higher spatial and temporal coverage in the northwestern Mediterranean than in the eastern basins particularly in the Adriatic Sea and the Levantine Basin. ~~Here, two major overturning circulation cells contribute to transporting carbon from the surface to the ocean interior (Lee et al., 2011). In the eastern Mediterranean, the northern and southern Adriatic play a key role in sustaining the thermohaline circulation (Robinson et al., 2001) and in capturing and storing CO_2 in the deeper layers (Cantoni et al., 2016; Ingrosso et al., 2017; Urbini et al., 2020; Cantoni et al., 2024). In particular, the Northern Adriatic Deep Water (NAdDW) represents the densest and most CO_2-rich water mass in the region, significantly contributing to deep ventilation and carbon sequestration in the eastern Mediterranean basin.~~

This observational gap highlights the need for sustained high-frequency measurements to better constrain surface carbon dynamics and air-sea CO_2 flux in these regions. In this study, a ~~new~~ recently validated in situ time series of sea surface observations from the EMSO-E2M3A South Adriatic regional facility and ICOS ERIC observatory (nominal position 41.5053°N, 18.0806°E), hereafter EMSO-E2M3A, is ~~presented~~discussed (Dentico et al., 2026). Time series of sea water partial pressure of CO_2 (pCO_{2sw}, µatm), hydrography and estimated CO_2 flux (FCO_2, mmol m^{-2} day^{-1}) are ~~discussed~~investigated. One of the major goals of this research is to assess the role of the S~~s~~outhern Adriatic (SAd) as a carbon sink or source in the last decade. To our knowledge, this is the first ~~time that a~~ comprehensive study on carbon dynamics and carbon flux in the ~~region~~ SAd ~~using~~ based on high resolution in situ observations ~~has been achieved~~. In addition, the effect of different wind forcings (in situ observations and reanalysis), varying in situ temporal resolutions, and alternative gas transfer velocity parametrizations on FCO_2 estimates are analysed. Further, it is shown how the SAd pCO_{2sw} and FCO_2 time series can be a key asset for biogeochemical reanalyses. ~~Considering the Mediterranean Copernicus Marine Service biogeochemical reanalysis~~, T~~t~~he SAd data allowed to validate the Mediterranean Copernicus Marine

Service biogeochemical reanalysis biogeochemical reanalyses representing a valid as a good tool to represent reconstruct local dynamics while highlighting the presence of some differences in the amplitude of seasonal cycles of both pCO_{2sw} and FCO_2.

The paper is organized as follows. Section 2 describes the study area, Section 3 describes the data used and the thermodynamic calculation performed to estimate carbon flux. Results are presented and discussed in section 4. Conclusions are provided in Section 5.

2. Study area

The Ssouthern Adriatic (SAd) is located between the Palagruža Sill and the Strait of Otranto, where maximum depth reaches about 1250 m in the Southern Adriatic Pit (SAP; Figure 1). This area is featured by a quasi-permanent cyclonic circulation, and it is well known that dense water formation takes place at the centre of the gyre through open-ocean convection (Ovchinnikov et al., 1985; Gačic et al., 2002; Mantziafou and Lascaratos, 2004; Chiggiato et al., 2016; Amitai et al., 2021) contributing to the eastern Mediterranean thermohaline circulation (Robinson et al., 2001).

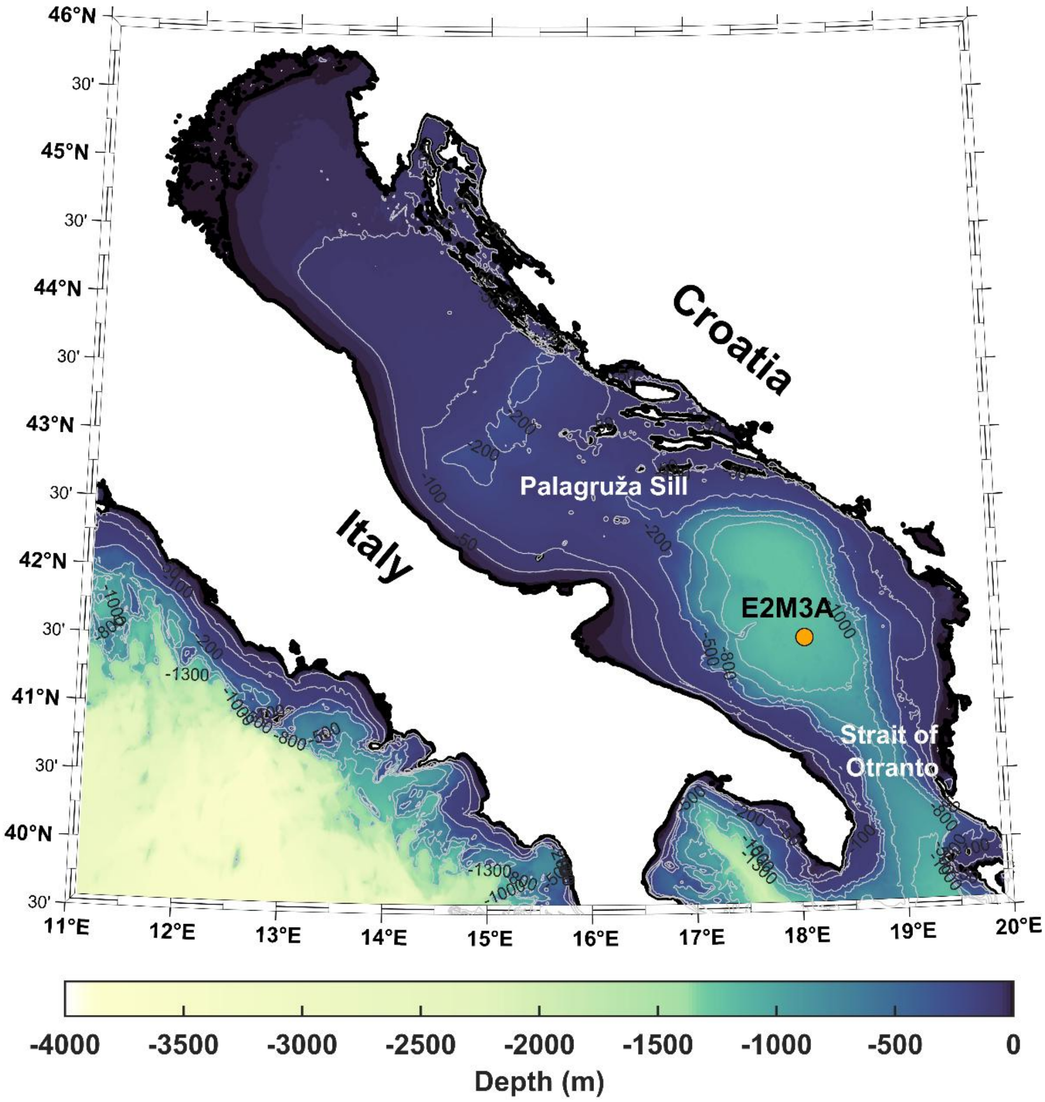

Figure 1. Map of the study area. The location of EMSO-E2M3A (nominal position 41.5053°N, 18.0806°E) moored at the center of the SAP is shown by the orange dot. The geographical boundaries of the Ssouthern Adriatic, i.e., the Palagruža Sill and the Strait of Otranto are also shown on the map. , are also displayed and highlighted by the two red lines.

The variability of physical and biogeochemical processes, including ocean carbon dynamics, is primarily related to the interaction of different water masses (Civitarese et al., 2023) and by deep convection processes (Ingrosso et al., 2017). The SAd is one of the main dense water formation regions of the eastern Mediterranean (Schlitzer et al., 1991; Roether and Schlitzer, 1991), where winter convection ventilates the water column. In addition to locally formed dense waters, the SAd also receives Northern Adriatic Dense Water, which is produced during winter on the northern Adriatic shelf and eventually enters the SAP (Cardin et al., 2011). On interannual timescales, the hydrographic variability of the SAd is further influenced by the Bimodal Oscillating System (BiOS), which modulates the properties of the intermediate waters entering the basin and results in alternating periods of fresher and colder Atlantic waters or saltier and warmer waters from the Ionian Sea (Gačić et al., 2010; Civitarese et al., 2010; Civitarese et al., 2023). Finally, the SAd is characterized by oligotrophic conditions, with relatively low biological productivity compared to other Mediterranean regions (Cerino et al., 2012; Matek et al., 2023).~~The Adriatic Dense Water (AdDW) occupies the bottom layer of the SAP and represents the main component of dense water for the whole Eastern Mediterranean basin (Schlitzer et al., 1991; Roether and Schlitzer, 1991). About 82 % of this water mass is formed through winter convection in the SAd (Ingrosso et al., 2017), while the remaining part has its origin on the northern Adriatic shelf and in the middle Adriatic Sea (Ovchinnikov et al., 1985; Bignami et al., 1990; Malanotte-Rizzoli, 1991). The Northern Adriatic Dense Water (NAdDW) is formed in the shallow northern Adriatic during winter, due to the cooling of the entire water column and of the evaporation caused by E-NE wind (named Bora). The process of formation of NAdDW is characterised by a high interannual variability as it is preconditioned by periods of low freshwater discharge by the rivers at least 4-5 months before its generation (Vilibić and Supić, 2005). These meteorological and oceanographic conditions also favour CO_2 and O_2 dissolution when surface water is undersaturated with respect to the overlying atmosphere. The CO_2 and oxygen enriched NAdDW is usually partially filling the middle Adriatic Pit and partly flows southward to the SAP (Cardin et al., 2011). On an interannual time scale, the physical and biogeochemical dynamics of the SAd is also strictly linked to that of the Ionian Sea (IS) by means of the Bimodal Oscillating System (BiOS). This mechanism changes the vorticity of the North Ionian Gyre (NIG) from cyclonic to anticyclonic and vice versa (Gačić et al., 2010; Civitarese et al., 2010; Civitarese et al., 2023). When the NIG is anticyclonic, the Modified Atlantic Water (MAW) coming from the Sicily Channel is in part deviated toward the northern Ionian and eventually enters the SAd, decreasing the salinity and the density of the AdDW. The change in the properties of the outflowing AdDW causes a progressive weakening of the anticyclonic upper-layer circulation in the IS. The circulation reverses, modifying the pathways of the water masses suppressing the northern branch of the MAW flow and favours the rapid advection of salty Levantine and/or Cretan Intermediate Water (LIW; CIW) along the eastern flank of the IS into the SAd. This results in an increase in the salinity (and density) of AdDW outflowing into the IS that gradually impairs the cyclonic NIG, eventually reversing it to an anticyclone. Finally, along the western coast in the SAd, the Adriatic Surface Water (AdSW) can be found. This is a relatively fresh and warm water mass, which originates from the northern Adriatic rivers runoff and flows southward along a narrow coastal layer of the western Italian shelf and exits through the Strait of Otranto.~~

The variability of the biogeochemical properties and the carbonate system of the SAd were almost continuously monitored by open ocean observatories, sampling activities and by ocean Argo floats and gliders. Particularly, the EMSO-E2M3A, which is located at the center of the SAP (Figure 1) and it is operated by the Italian National Institute of Oceanography and Applied Geophysics (OGS), represents a key research infrastructure to study biogeochemical and hydrographical properties of the whole water column in the SAP. EMSO-E2M3A is part of the European Multidisciplinary Seafloor and water column Observatory (EMSO) and the ~~ICOS (~~Integrated Carbon Observation System (ICOS)~~)~~ and the ~~ERIC~~ European Research Infrastructure Consortium (ERIC) networks. It consists of a system of two moorings, with the main mooring housing the surface buoy and ~~it is~~ equipped with a meteorological station and radiometers, sensors for physical (hydrography) and chemical variables ($p\mathrm{CO}_{2\mathrm{sw}}$, dissolved oxygen and pH), telemetry and services (Ravaioli et al., 2016). The secondary mooring line is composed of an instrument chain with sensors at different depths for physical and chemical measurements from the seafloor to the intermediate layer (Cardin et al., 2025a). The station has been in operation almost continuously since 2006 and is the longest open sea time series in the Adriatic. Additional information on EMSO-E2M3A, such as the scheme of the surface buoy and of the deep mooring with the depths of the different instruments, are described in Dentico et al. (2026).

3. Data and Methods

3.1. In situ sea surface $p\mathrm{CO}_2$ and CTD data ~~In situ measurements~~

The time series of $p\mathrm{CO}_{2\mathrm{sw}}$ (µatm) ~~and hydrological variables~~ presented in this study were measured by different Pro-Oceanus CO2 sensors at the EMSO-E2M3A at a depth of approximately 2 m (Cardin et al., 2025b). ~~A ProOceanus CO_2 sensor provided autonomous high-frequency (every four hours) measurements of~~ High frequency (every four hours) $p\mathrm{CO}_{2\mathrm{sw}}$ measurements spanned over a period ~~(µatm)~~ from 2015 to 2024 with declared accuracy of ± 0.5%~~5 µatm~~. This time series was complemented with $p\mathrm{CO}_{2\mathrm{sw}}$ measurements collected around the EMSO-E2M3A in July 2020 by an Uncrewed Surface Vehicle (USV, Saildrone Inc., USA) during the ATL2MED demonstration experiment (Martellucci et al., 2024a, 2025). Additionally, SOCAT V2026 observations in the SAd were included in the $p\mathrm{CO}_{2\mathrm{sw}}$ time series showed here. This data covers three years of observation in 2015 (August and September), in 2016 (August and September) and 2020 (June and July) with the latter corresponding to the ATL2MED demonstration experiment data. Hourly sea surface temperature (SST, °C), salinity (Sal) and dissolved oxygen (DO, µmol kg^{-1}) were measured by a SeaBird SBE 37-ODO with declared accuracy of ± 0.002 °C, ± 0.003 mS cm^{-1}, ± 0.1 % full scale range, respectively. DO from SBE 37-ODO was also used to calculate the apparent oxygen utilization (AOU, µmol kg^{-1}). This value corresponds to the difference between the equilibrium saturation of oxygen concentration in seawater with the same physical and chemical properties and the measured oxygen concentration, providing an estimation of the balance between primary production and respiration. AOU has been computed using the solubility coefficients from Benson and Krause (1984) as fitted by Garcia and Gordon (1992). A detailed description of the dataset used here and the quality control procedures applied to the data are available in Dentico et al. (2026~~5~~).

3.2. In situ atmospheric $p\mathrm{CO}_2$ data

To calculate air-sea FCO_2, hourly atmospheric molar fraction of CO_2 (xCO_2, ppm) from the ENEA (Italian National Agency for New Technologies, Energy and Sustainable Economic Development) Station for Climate Observations on the island of Lampedusa (Marullo et al., 2021; di Sarra et al., 2025) were used. Indeed, atmospheric pCO_2 measurements (pCO_{2atm}, µatm) at EMSO-E2M3A only started in December 2023, when a ProOceanus CO_2-Pro ATM was deployed allowing continuous measurements of both pCO_{2sw} and pCO_{2atm} in alternating mode. As in situ observations of pCO_{2atm} were not long enough to match with pCO_{2sw}, Lampedusa data was chosen as it represents one of the longest oceanic time series of pCO_{2atm} in the Mediterranean Ssea. Moreover, these data have been used in similar studies to compute FCO_2 at Mediterranean scale (e.g., Martellucci et al., 2024a; 2025) and in the northern Adriatic Sea (e.g., Urbini et al., 2020; Cantoni et al., 2024). From Lampedusa xCO_2 (indicated as xCO_{2_LMP}), the pCO_{2atm} relative to the local physical and atmospheric condition at EMSO-E2M3A (indicated as pCO_{2atm_E2M3Ar}) was calculated according to Weiss et al., (1974):

$$pCO_{2atm\_E2M3Ar} = xCO_{2\_LMP}\,(P - pH_2O) \qquad (1)$$

where P is the air pressure (mbar) measured at EMSO-E2M3A and pH_2O (mbar) is the water vapour saturation that has been calculated according to Weiss and Price (1980):

$$pH_2O = Aexp^{(B - C(100/SST) - Dlog(SST/100) - E(SSS))} \qquad (2)$$

where SST is sea surface temperature (K), SSS is sea surface salinity both measured at EMSO-E2M3A and the coefficients A, B, C and D can be found in Weiss and Price (1980). To assess the potential bias of using xCO_{2_LMP} for the calculation of CO_2 air-sea flux in the SAd, a comparison between pCO_{2atm} measured by the ProOceanus CO_2-Pro ATM sensor installed at EMSO-E2M3A (pCO_{2atm_E2M3A}) with pCO_{2atm_E2M3Ar} was performed. This comparison was limited to a four-month period between December 2023 and March 2024, when the CO_2-Pro ATM sensor was operational. The two time series show good overall agreement, however the differences tend to be larger at higher pCO_{2atm} values, while they remain smaller at lower values (Fig. S1, S2a, Supplementary Material). A mean difference of +2.767 ± 3.15 µatm between pCO_{2atm_E2M3A} and pCO_{2atm_E2M3Ar} indicate that pCO_{2atm_E2M3A} is on average higher than pCO_{2atm} derived from xCO_{2_LMP}. A detailed investigation of the reasons behind this difference was beyond the scope of this work. Although the analysis of the residuals indicated potential heteroscedasticity in the data (Fig. S2a, S2b, Supplementary Material), the short duration of the overlapping time series justified applying a constant bias correction of + 2.767 µatm to pCO_{2atm_E2M3Ar}. To evaluate the robustness of this correction, a comparison between pCO_{2atm} derived from the CAMS reanalysis of the European Centre for Medium-Range Weather Forecasts (ECMWF; Agustí-Panareda et al., 2023), was also considered (Figure S3, Supplementary Material). The difference between monthly

pCO$_{2atm}$ data at Lampedusa (LMP) and at EMSO-E2M3A between 2003 and 2021 was 2 ppm which is similar to the offset estimated in the four-month period.

3.3. In situ wind speed data

~~Finally, w~~Wind speed (WSPD, m s^{-1}) was measured by a Young sensor on the meteorological station at EMSO-E2M3A (Cardin et al., 2025b; Dentico et al., 2026~~5~~) with a manufacturer accuracy of ± 0.3 m s^{-1} and was used as input for CO_2 flux calculation. Given that at EMSO-E2M3A wind speed is measured at 2 m height and CO_2 air-sea flux calculation requires the standard reference height of 10 m (Wanninkhof, 2014), a conversion was performed using a logarithm wind speed profile according to:

$$u_{LOG(z)} = (ln(z/z_0) \,/\, ln(z_m/z_0))u_{(zm)} \quad (3)$$

where $u_{LOG(z)}$ is the wind speed (m s^{-1}) at the desired height (10 m), z is the desired measurement height (10 m), z_m the actual measurement height (2 m), z_0 is the roughness length that for oceanic regions was set equal to 1.52 x 10^{-4} (Peixoto and Ort, 1992) and $u_{(zm)}$ is the wind speed (m s^{-1}) measured at EMSO-E2M3A at 2 m height. A detailed description of the data collection and quality check of the data can be found in Dentico et al. (2026).

3.4~~2~~. Model data

The European~~EU~~ Copernicus Marine Service (CMEMS) provides regular and systematic information on the ocean physics and biogeochemistry for the global ocean and the European regional seas (Le Tra~~e~~on et al. 2019). Data from different Mediterranean CMEMS products were used as an additional reference to investigate the variability of the in situ pCO$_{2sw}$ and FCO$_2$. In particular, the following modelling products were used: the Sea Physics Reanalysis (PHY, Escudier et al., 2021) for the physical variables of surface temperature (SST, °C), salinity (Sal) and Mixed Layer Depth (MLD, m), the Biogeochemistry Reanalysis (RD; Cossarini et al., 2021) and the Biogeochemistry Analysis and Forecast product (AF; Salon et al., 2019) for pCO$_{2sw}$ (µatm~~mt~~) and FCO$_2$ (mmol m^{-2} day^{-1}). Additionally, the Ocean Color Satellite product (Volpe et al., 2019) for~~of~~ the surface chlorophyll-a (Chl-a, µg l^{-1}) was used as a proxy of primary production. Detailed information on the models and variables used are summarized in Table 1. The time series presented here are spatial averages of the grid points in the 10 km radius from EMSO-E2M3A from the native spatial resolution of 4.5 km and 1 km for models and satellite data, respectively.

Table 1. Overview of the Copernicus Marine Service (CMEMS) products used in this work.

CMEMS product name	Variables used in this work	DOI	Reference
Mediterranean Sea Physics Reanalysis (PHY)	SST, Sal, MLD	https://doi.org/10.25423/CMCC/MEDSEA_MULTIYEAR_PHY_006_004	Escudier et al., (2021)
Mediterranean Sea Biogeochemistry Reanalysis (RD)	$p$$CO_{2sw}$, FCO_2	https://doi.org/10.25423/cmcc/medsea_multiyear_bgc_006_008_medbfm3	Cossarini et al., (2021)
Mediterranean Sea Biogeochemistry Analysis and Forecast (AF)	$p$$CO_{2sw}$, FCO_2	https://doi.org/10.25423/cmcc/medsea_analysisforecast_bgc_006_014_medbfm4	Salon et al., (2019)
Mediterranean Sea, Bio-Geo-Chemical, L4, monthly means, daily gapfree and climatology Satellite Observations (1997-ongoing)	Chl-a	https://doi.org/10.48670/moi-00300	Volpe et al., (2019)

ERA5 wind product, which is the fifth generation of ECMWF reanalysis for the global climate and weather (Hersbach et al., 2023), was also used and compared with EMSO-E2M3A wind measurements. ERA5 provides hourly estimates for a large number of atmospheric, ocean-wave and land-surface quantities from 1940 to present. The spatial resolution of atmospheric data is 0.25° x 0.25° and wind speed ($WSPD_{ERA5}$, m s^{-1}) in the subregion close to EMSO-E2M3A (30 km radius) and in the nearest point close to EMSO-E2M3A was calculated as the square root of the sum of square of the 10 m u-component (m s^{-1}), which is the eastward horizontal wind speed, and the square of the 10 m v-component (m s^{-1}) that represents the northward horizontal wind speed. according to the following:

(4)

where is the square of the 10 m u-component (m s^{-1}), which is the eastward horizontal wind speed, while is the square of the 10 m v-component (m s^{-1}) that represents the northward horizontal wind speed. ERA5 wind speed data were selected for two main reasons: (i) wind reanalysis products, unlike in situ time series, provide continuous spatial and temporal coverage without observational gaps; (ii) ERA5 wind data are used as the wind forcing input in the Mediterranean Sea Physical and Biogeochemistry Reanalyses. Thus, considering that CO_2 air-sea flux in the CMEMS products and in the present work was computed following the same formulation (Wanninkhof, 2014), the use of the

~~same wind dataset, allowed a focus on the analyses of pCO_{2sw} difference between in situ data and model outputs. Nevertheless, a validation of the ERA5 wind data using local wind conditions at EMSO-E2M3A and a discussion on the uncertainties introduced by the use of ERA5 data in computing FCO_2 will be presented.~~

3.5~~3~~. ~~Thermodynamic~~ Air-sea CO_2 flux calculation~~s~~

The direction and magnitude of FCO_2 is governed by the difference between pCO_{2sw} and pCO_{2atm} and the air-sea CO_2 gas transfer velocity (Takahashi et al., 2002):

$$FCO_2 = k_0 k(pCO_{2sw} - pCO_{2atm}) \quad (~~5~~4)$$

where k_0 is the solubility coefficient of CO_2 at in situ temperature and salinity (Weiss, 1974; Zeebe and Wolf-Gladrow, 2001) and k is the gas transfer velocity (m day^{-1}). In this study, if the $FCO_2 < 0$ the flux is from air to seawater, on the contrary if $FCO_2 > 0$ the flux is from the seawater to the atmosphere. Several algorithms for k calculation exists, here different parametrizations were used to compute FCO_2: ~~the parametrization proposed by Wanninkhof (2014) was used:~~

$$~~k~~ k_W = 0.251u^2(Sc/660)^{-0.5} \quad (~~6~~5)$$

$$k_{W\&McG} = 0.0283u^3(Sc/660)^{-0.5} \quad (6)$$

$$k_N = 0.222u^2 + 0.333u(Sc/600)^{-0.5} \quad (7)$$

where k_W is a quadratic relationship proposed by Wanninkhof (2014) and it is one of the most frequent parametrizations used in the FCO_2 estimations at both global and Mediterranean scale (Urbini et al., 2020; Cantoni et al., 2024; Martellucci et al., 2025; Pecci et al., 2026); ~~where u is the 6-hourly wind speed averages (m s^{-1}) at 10 m height and Sc the Schmidt number for CO_2. Wanninkhof (2014), hereafter W14, has been proved to best represent the relationship between wind speed and gas exchange at a regional-to-global scale. For instance it was used in similar studies in the Mediterranean Sea (Pecci et al., 2024; Martellucci et al., 2025) and in the Adriatic basin (e.g., Urbini et al., 2020; Cantoni et al., 2024).~~ $k_{W\&McG}$ is a cubic wind speed dependencies from Wanninkhof and McGillis (1999); and k_N is a mixed (linear and quadratic) dependency from Nightingale et al. (2000) used in literature (for example in Gulf of Biscay; Otero et al., 2013). In Eq. (5), (6) and (7) u is the wind speed (m s^{-1}) corrected at 10 m height and Sc the Schmidt number for CO_2. Different temporal resolutions of u have been used to compute Eq. (5), (6) and (7) including hourly, 6-hours averages and daily averages. From these, daily k values have been calculated to have daily FCO_2 values. Additionally, 6-hours averages ERA5 wind speed data have been used to calculate the different parametrizations of *k*. ERA5 wind speed data were selected for two main reasons: (i) wind reanalysis products, unlike in situ time series, provide continuous spatial and temporal coverage without observational gaps; (ii) ERA5 wind data are used as the wind forcing input in the Mediterranean Sea Physical and Biogeochemistry Reanalyses. Thus, considering that CO_2 air-sea flux in the CMEMS products (Salon et al., 2019; Cossarini et al., 2021) and in the present work was computed following the same Wanninkhof (2014) formulation, the use of the same wind dataset, allowed a focus on the analyses of pCO_{2sw} difference between in situ data and model outputs. In summary, different wind products (EMSO-E2M3A versus ERA5), different formulation of *k* and different temporal resolution were used to compute the FCO_2 and to assess their impact on annual and seasonal estimates. ~~Acknowledging that W14 provides the best fit with the Cross-Calibrated Multi-Platform (CMPP) wind product (Atlas et al., 2011), this formulation was applied using wind speed measurements from EMSO-E2M3A and from ERA5. This choice ensures methodological consistency in the comparison between CO_2 flux calculated from in situ data and those from the models.~~

3.4. Thermal and non thermal component of pCO_{2sw}

Thermal (pCO_{2sw_T}, µatm) and non-thermal (pCO_{2sw_NT}, µatm) components of pCO_{2sw} were estimated according to Takahashi et al. (2002). The thermal component is associated to the effect of temperature on pCO_{2sw}, while the non-thermal component can be attributed to other factors not strictly related to temperature, as biological activity (photosynthesis and respiration), changes in dissolved inorganic carbon ~~(DIC)~~, mixing or advective processes and gas exchange with the atmosphere. pCO_{2sw_T} and pCO_{2sw_NT} have been computed using the following equations:

$$pCO_{2sw\_T} = mean(pCO2_{sw}) exp^{0.0423(SST_{obs} - SST_{mean})} \quad (~~7~~8)$$

$$pCO_{2s\_NT} = pCO2_{sw} exp^{0.0423(SST_{mean} - SST_{obs})} \quad (~~8~~9)$$

where, *mean* refers to yearly mean values of sea surface temperature (SST, °C), while the other variables (pCO_{2sw} and SST_{obs}) refer to the daily values measured during the study period.

4. Results and Discussion

4.1. pCO_2 dynamics and hydrography in the SAP

The time series of the daily surface pCO_{2sw} between 2015 and 2024 is presented in Fig. 2a. The incomplete coverage of the full seasonal cycle in several years, prevented a detailed assessment of interannual variability. Therefore, the discussion presented in this section mainly focuses on the seasonal patterns and its main drivers, and, when possible, on interannual differences of the seasonal cycle.

Mean winter values were around 380 µatm and mean summer values reached around 484 µatm, resulting in a seasonal amplitude of about 100 µatm. This pronounced seasonality reflected the combined influence of thermal and non-thermal processes (Fig. 2b). During winter, low sea surface temperature (SST < 15 °C; Fig. 2c)~~Fig. 2b~~) increases CO_2 solubility, leading to lower pCO_{2sw} (Fig. 2b). However, during winter convection the upward transport of DIC-rich intermediate and deep waters (Touratier et al., 2016; Ingrosso et al., 2017) led to an increase of surface pCO_{2sw} ~~during winter convection, vertical mixing increased surface pCO_{2sw},~~ as shown by the pCO_{2_NT} component (Fig. 2b~~a~~). This was particularly evident between late December and late February of 2016–2017, 2017–2018, 2020–2021, and 2023–2024 (Fig. 2a). ~~These increases were particularly evident between late December and late February of 2016–2017, 2017–2018, 2020–2021, and 2023–2024 (Fig. 2a)~~. ~~As described in Touratier et al. (2016) and in Ingrosso et al. (2017), vertical convection brings intermediate/deep CO_2-rich waters to the surface, causing increases in surface pCO_{2sw}.~~ Positive AOU values observed during these periods (Fig. 2d~~e~~) further support this interpretation, indicating the ~~confirmed the occurance of vertical mixing – the~~ upward displacement of oxygen-depleted intermediate waters during vertical mixing, ~~as~~ also described ~~also~~ in Martellucci et al. (2024b). The post-convection periods (usually from March to May-June) were characterised by a phytoplankton bloom (Fig. 2f~~e~~). Although direct pCO_{2sw} observations were limited during this period, the decrease in AOU and the increase in DO concentration at the surface (Fig. 2d) provided indirect but consistent evidence of primary production. These observations suggest that biological CO_2 uptake likely contributes to lowering pCO_{2sw} following winter mixing, acting as an additional non-thermal driver of the seasonal variability. ~~, but its direct effect on pCO_{2sw} was less clear as few data were available in these periods. However, photosynthesis during the bloom, as suggested by negative AOU values and an increase in oxygen concentrations at the surface (Fig. 2e), could likely contribute to decreasing pCO_{2sw}.~~ In spring, surface warming began, leading, in summer, to maximum SST values (> 25 °C; Fig. 2c) and strong stratification. During this period, pCO_{2sw} reached its annual maximum, closely following the pCO_{2sw_T} component and indicating a ~~strong~~ dominant thermal effect (Fig. 2b~~a~~). ~~Independent measurements from an Unmanned Surface Vehicle (USV) operating in the area in July 2019 during the ATL2MED experiment (Martellucci et al., 2025)~~ The comparison between the Saildrone and EMSO-E2M3A observations further confirmed this pattern, showing coherent short-term variations with the EMSO-E2M3A time series ~~,~~ (r = 0.77, p value < 0.01) and a nearly constant offset of 16 µatm (Fig. 2a). Similarly, SOCAT V2026 observations showed very good agreement with the EMSO-E2M3A measurements during August–September 2015, (mean difference of approx. 8.4 µatm, Fig. 2a). In contrast, larger differences (mean difference approx. 40 µatm) were observed during the same period in 2016. The SOCAT observations in 2016 are located along the eastern side of the SAd, therefore, the discrepancies may reflect differences in the hydrographic conditions and water mass distribution between the two surveys, resulting in the sampling of waters with different physical and biogeochemical characteristics. However, further analyses would be required to confirm this hypothesis. Interestingly, higher pCO_{2sw} values were recorded in summer

2022, with a peak in July 2022, coinciding with the occurrence of a Mediterranean Marine Heatwave ~~(MHW)~~. In the SAP, Pirro et al. (2024) detected positive temperature anomalies across the whole water column, with the strongest warming at the surface. Thus, the elevated pCO_{2sw} observed in this period might be linked to ~~the MHW,~~ the increased stratification that limited vertical exchange favouring the accumulation of respired carbon in surface waters. This behaviour was consistent with recent observations in the northwestern Mediterranean Sea (e.g., Metzl et al., 2025), which highlighted that the exceptional warming observed in summer 2022 impacted not only thermodynamic processes but also stratification, wind field (Pecci et al., 2026) and biological activity, with consequences for the variability of pCO_{2sw} and air–sea CO_2 flux.

~~although further analyses, for instance in relation to wind change patterns (e.g., Pecci et al., 2024) would be required to confirm this hypothesis.~~ The annual cycle of surface pCO_{2sw} in the SAd was comparable to other regions of the Mediterranean Sea with generally lower values than those observed in the SAd (Dentico et al., 2026~~5~~). Similar seasonal variations especially in winter were described for the northern Adriatic shelf (Ingrosso et al., 2016; Urbini et al., 2020; Cantoni et al., 2024), where intense Bora wind events and vertical mixing periodically disrupt water column stratification, promoting an efficient exchange between bottom and surface pCO_{2sw}. Seasonal pCO_{2sw} variability was reported between 200 µatm in winter up to 500 µatm in summer (e.g., Cantoni et al., 2024). However, unlike the SAd, the riverine inputs in this area also play a key role in modulating the carbonate system dynamics (e.g., Giani et al., 2023). In the convective region of the northwestern Mediterranean Sea, several studies have emphasized the importance of vertical mixing, horizontal advection and biological productivity in driving pCO_{2sw} variability (e.g., Merlivat et al., 2018; Fourrier et al., 2022; Ulses et al., 2023). Here winter values were comparable to the SAd (around 350 µatm) and summer values around 500 µatm (Merlivat et al., 2018; García-Ibáñez et al., 2024) or higher, as reported for the DYFAMED site in the Ligurian Sea (Coppola et al., 2020) where values exceeded 550 µatm. In the SAd the effect of biological activity was less clear because of data gaps. Nevertheless, further investigations could be essential to clarify the role of biological processes in shaping the local carbon cycle as highlighted in previous studies (~~Socal~~ Turchetto et al., 2012; Cerino et al., 2012). ~~Finally, in n~~Non-convective regions such as the eastern Mediterranean Sea, exhibited a stronger thermal control on seasonal pCO_{2sw} variability. The first pCO_{2sw} time series from the Cretan Sea ~~(Frangoulis et al., 2024)~~showed that temperature was the dominant driver of pCO_{2sw}, while the non-thermal component was mainly associated with evaporation, water mass mixing, and biological remineralisation-production processes (Frangoulis et al., 2024). Similarly, in the southeast Levantine, seasonal pCO_{2sw} was found to be tightly correlated with sea surface temperature indicating that its seasonal cycle is largely controlled by thermodynamic processes (Sisma-Ventura et al., 2017).~~,~~ ~~or the Lampedusa site (Pecci et al., 2024), other processes appear to control pCO_{2sw} variability.~~ In contrast to the Levantine Basin, where pCO_{2sw} variability is strongly influenced by warming and evaporation, the Southern Adriatic is affected by recurrent deep convection and higher biological activity (e.g., Pérez et al., 2024; Tsiaras et al., 2024). Nevertheless, seasonal variations were similar ranging between 350 µatm in winter and around 500 µatm in summer (Frangoulis et al., 2024).

The analysis of hydrological data showed the highly dynamic characteristics of the region. First, the intensity and occurrence of convection in the SAd has varied substantially among years (Fig. 2fd). Depending on atmospheric forcing and water column preconditioning, the depth of vertical mixing ranged from relatively shallow mixing in the intermediate layers (< 400 m depth) to deeper convective events (> 800 m depth). Weaker events were recorded in 2015, 2016, 2019, and 2020, whereas deeper mixing (> 600 m) occurred in more recent years (especially after 2022; Fig. 2f). These interannual variabilityThis interannual variability resulted from strong/weak air-sea interactions, where stronger heat losses could occur especially under the influence of the cold and dry Bora wind (Le Meur et al., 2025). Variations in the regional hydrographic structure, particularly changes in salinity (Amorim et al., 2024; Le Meur et al., 2025), also affected the stability of the water column and the depth of convection. This variability in salinity (Fig. 2g) was associated with the inflow of Levantine/Ionian surface water, which is regulated by changes in the Northern Ionian Gyre (NIG) vorticity (Gačić et al., 2010; Rubino et al., 2020; Menna et al., 2022; Civitarese et al., 2023). The influence of NIG in the SAd was evident in the salinity measurements (Fig. 2gf), which showed periods of higher salinity (> 39 in 2017, 2021, 2022) and lower salinity (< 38.5 in 2015, 2018). Through its impact on stratification and preconditioning, this large-scale circulation variability likely modulates the intensity of winter mixing and, indirectly, pCO_{2sw} variability.

501 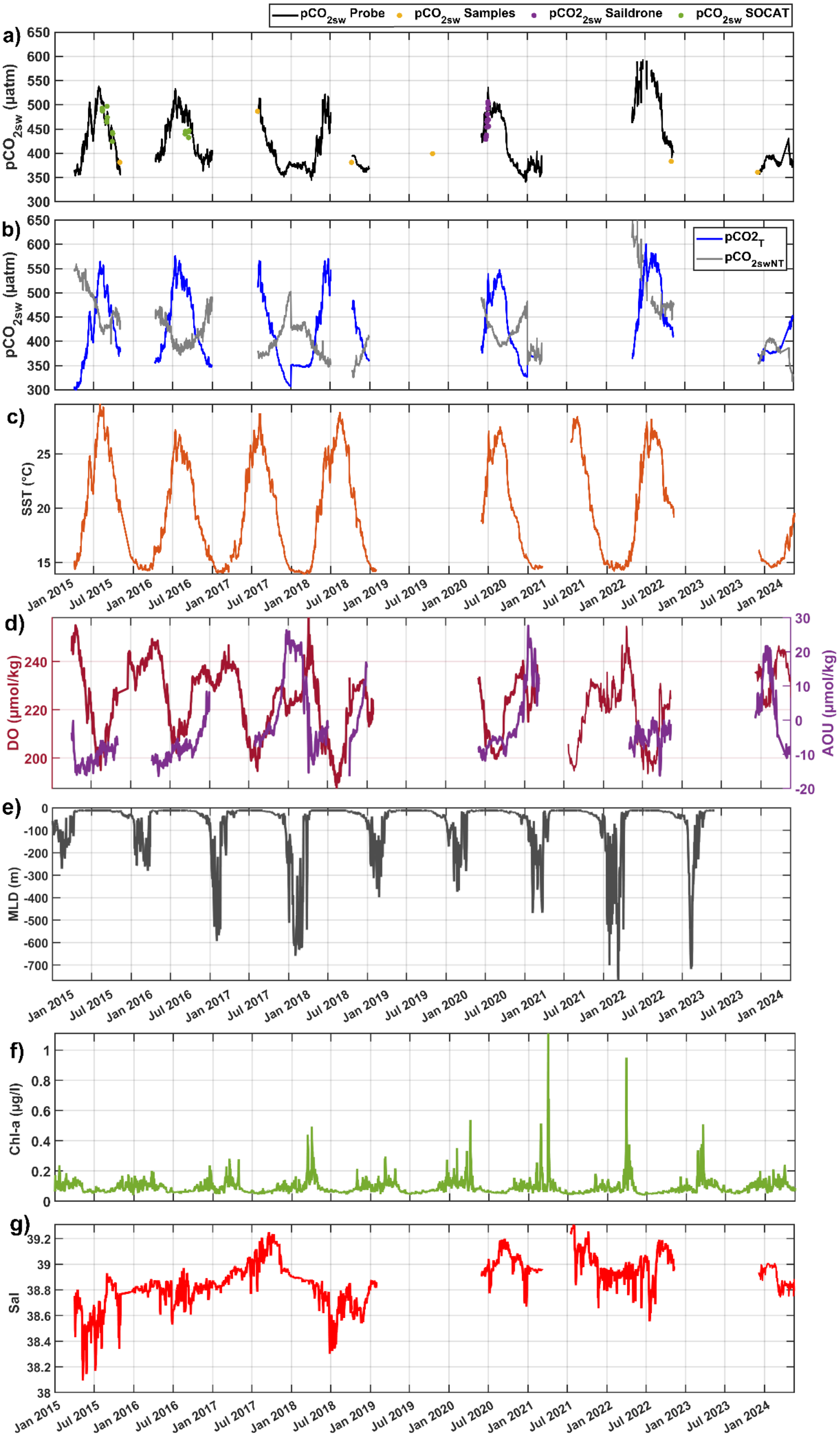
pCO2sw Probe
pCO2sw Samples
pCO22sw Saildrone
pCO2sw SOCAT
a)
pCO2sw (µatm)
b)
pCO2T
pCO2swNT
c)
SST (°C)
d)
DO (µmol/kg)
AOU (µmol/kg)
e)
MLD (m)
f)
Chl-a (µg/l)
g)
Sal
Jan 2015
Jul 2015
Jan 2016
Jul 2016
Jan 2017
Jul 2017
Jan 2018
Jul 2018
Jan 2019
Jul 2019
Jan 2020
Jul 2020
Jan 2021
Jul 2021
Jan 2022
Jul 2022
Jan 2023
Jul 2023
Jan 2024

Figure 2. Time series of daily a) Partial pressure of CO_2 in seawater (pCO_{2sw} Probe, µatm) measured by the Pro-Oceanus sensor represented by the black solid line, partial pressure of CO_2 in seawater derived from the analysis of water samples using the pair pH and total alkalinity (pCO_{2sw} Samples, µatm), partial pressure of CO_2 in seawater measured by the Saildrone (pCO_{2sw} Saildrone, µatm), and partial pressure of CO_2 in seawater from SOCAT in the SAd (pCO_{2sw} SOCAT, µatm) represented by the yellow, violet and green dots respectively; b) ~~and the t~~Thermal (pCO_{2_T}, µatm) and non thermal (pCO_{2_NT}, µatm) components of pCO_{2sw} (µatm) ~~in black,~~ blue and grey~~,~~ respectively; c~~b~~) Sea surface temperature (SST, °C); d~~c~~) Dissolved oxygen (DO, µmol kg^{-1}) and Apparent Oxygen Utilization (AOU, µmol kg^{-1}) derived from DO measured by the SBE37 ODO sensor in dark red and violet respectively; e~~d~~) Mixed Layer Depth (MLD, m) from the CMEMS Mediterranean Sea Physics Reanalysis; f~~e~~) Chlorophyll-a (Chl-a, µg l^{-1}) used here as a proxy of primary production from the CMEMS Mediterranean Sea, Bio-Geo-Chemical, L4, monthly means, daily gapfree and climatology Satellite Observations (1997-ongoing); and g~~f~~) Sea surface salinity (Sal). Time series (a, b, c and f) refers to the data measured by several instruments deployed at 2 m depth at EMSO-E2M3A between April 2015 and May 2024. Data gaps in the series were mostly due to maintenance operations and/or discarded data because they failed the quality-control procedures described in Dentico et al. (2026~~5~~). Modified from Dentico et al. (2026~~5~~).

4.2. CO_2 flux: source-sink dynamics

Daily FCO_2 in the SAd ~~presented in this section~~shown in Fig. 3 ~~has been~~were ~~-~~computed using a reference configuration based on ~~according to~~ Eq. (~~5~~4) and Eq. (~~6~~5) using as input pCO_{2sw}, pCO_{2atm_E2M3Ar} (Sect. 3.1) and 6-hours averaged wind speed data from EMSO-E2M3A corrected at 10 m height (Sect. 3.3). The gas transfer velocity was calculated using the Wanninkhof (2014) parameterisation to allow a more consistent comparison with previous studies and model data (Sect. 4.4). FCO_2 estimates obtained using different wind products, wind temporal resolutions, and gas transfer velocity parameterisations are discussed in Sect. 4.3. Based on the reference configuration, CO_2 air-sea flux in the SAd presents two dominant phases: a source period, generally associated with post-convection/summer months (positive values in Fig. 3a), and a sink period, typically occurring during winter and during episodes of winter convection (negative values in Fig. 3a). While the intensity of daily values during sink and source phases exhibited high interannual variability, the timing of the transition months, i.e., the periods when the SAd shifts from a source (May) to a sink (October), occurred regularly (Fig. 3b).

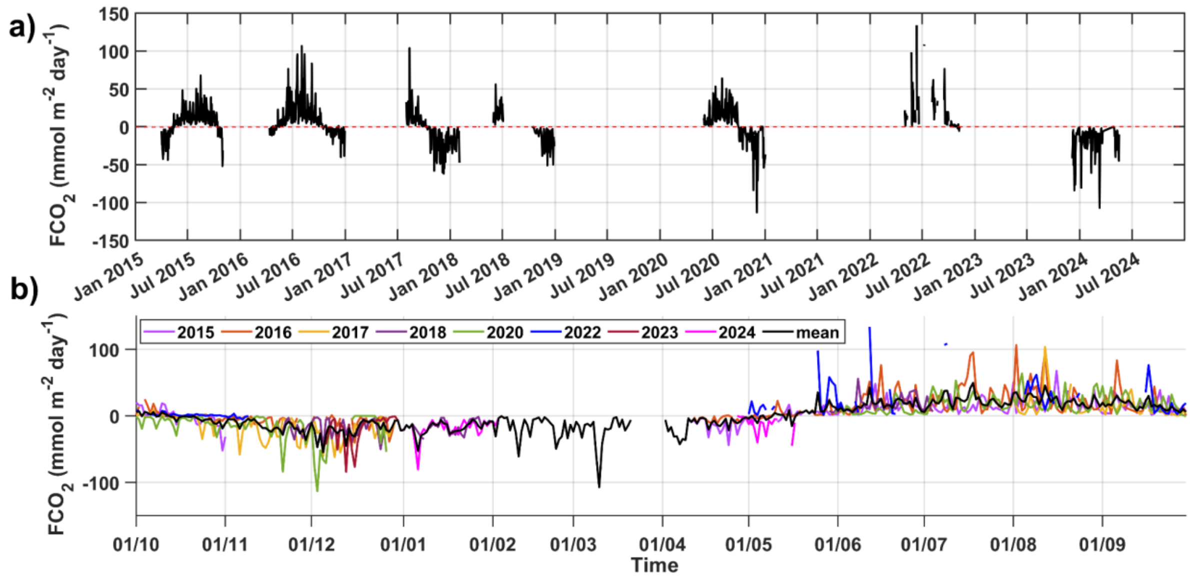

Figure 3. a) Time series of daily CO_2 flux (FCO_2, mmol m^{-2} day^{-1}) calculated with in situ measurements in the period 2015-2024 at EMSO-E2M3A; b) Daily averages of CO_2 flux calculated in the different years (coloured lines) and the mean daily FCO_2 (mmol m^{-2} day^{-1}) over the entire period (2015-2024; black line). Negative flux represents CO_2 influx from the air to the sea and positive flux represents CO_2 outgassing from the sea to the air.

Monthly averages were computed for those months with at least 14 valid daily values. The mean over the full period was subsequently obtained from these monthly values (Fig. 3b). Given the observed variability (i.e., high daily variability with a regular annual cycle) and the presence of substantial data gaps in the FCO_2 time series, ~~two complementary~~an additional computational approaches ~~were~~ was applied to derive robust estimates of mean CO_2 fluxes in the SAP over the past decade (Table S1~~,~~ Supplementary Material). ~~By considering two different orders in the process of aggregating data for computing averages, the sensitivity of data sampling irregularity to the overall mean was verified. In the first approach (hereafter M1), the daily means for each day of the year were calculated. Outliners were then identified and removed through visual inspection, with particular attention to values not supported by a sufficiently large number of observations. Finally, monthly means were derived, and the overall mean for the entire study period (2015-2024) was computed from the 12 monthly averages. In the second approach (hereafter M2), a 2015-2024 time series of the monthly values is computed for those months with at least 14 valid daily values. The mean over the full period was subsequently obtained from these monthly values. A summary of the monthly means obtained with M1 and M2 is reported in Table 2.~~

~~**Table 2**. Monthly mean of FCO_2 (mmol m^{-2} day^{-1}) in the SAd calculated with in situ data from the EMSO-E2M3A regional facility in the period 2015-2024 using two different computation methods. Relative difference was calculated as M1 – M2 divided by M1.~~

Month of the year	M1 (mmol m^{-2} day^{-1})	M2 (mmol m^{-2} day^{-1})	M1 - M2	Relative difference
January	-17.92	-17.89	-0.04	0.0020
February	-16.75	-15.96	-0.78	0.0469
March	-12.79	-12.79	0.00	0.0000
April	-14.26	-11.02	-3.23	0.2269
May	6.36	9.80	-3.44	-0.5410
June	16.67	16.31	0.36	0.0215
July	22.49	21.06	1.43	0.0635
August	24.11	22.90	1.22	0.0504
September	15.61	15.58	0.03	0.0017
October	-1.99	-1.88	-0.11	0.0577
November	-15.30	-15.62	0.32	-0.0209
December	-20.14	-19.69	-0.45	0.0222

Both methods produced consistent results, with an average difference of approximately 5 % between M1 and M2. The largest discrepancies between the two methods occurred in April and May. In April these can be due to the lower data availability (Fig. 3b), as only two years of data were available. On the contrary, in May a transition between source and sink conditions occurs, thus explaining the larger differences between M1 and M2. Similarly, in February, data for only one year (2024) was available throughout the month with the addition of a few days at the beginning of February 2018 making this approach not robust enough to have reliable results (higher difference between M1 and M2). Finally, in March data were available only in 2024, and the proposed aggregating processes produced no difference between M1 and M2. Notwithstanding these potential limitations derived by data availability, the results indicated that, over the last decade, the SAd has functioned predominantly as a weak-to-moderate carbon sink. For the period 2015-2024, with mean annual FCO_2 values of about -0.97 ranged from -1.15 mmol m^{-2} day^{-1} (M1) to -0.76 mmol m^{-2} day^{-1} for the period 2015-2024(M2). Across the Mediterranean, air-sea carbon flux is spatially uneven: the western basin takes up more CO_2 than the eastern basin, while some southeastern sectors show weak release or near-neutral behaviour (Cossarini et al., 2021). Although the values reported here for the SAd were modest in magnitude compared to other Mediterranean regions, they these values consistently pointed to a net CO_2 uptake, underscoring the potential role of the SAd in regional carbon sequestration, as suggested by Ingrosso et al. (2017). While the present analysis does not directly address the carbon export below the mixed layer, the occurrence of recurrent convection events suggests that part of the CO_2 absorbed at the surface may be transferred to intermediate and deep waters. In this context, our results are consistent with observations from other Mediterranean deep-water formation ~~Further, these results confirm the role of dense water formation sites as primary drivers of carbon sequestration. Indeed,~~regions. For instance, the northern Adriatic Sea has been reported to act as an effective CO_2 sink during winter, spring, and autumn, with mean daily fluxes of about -2.9 mmol m^{-2} day^{-1} (Catalano et al., 2014; Cantoni et al., 2024) reaching however the highest CO_2 flux during winter (-14.2 mmol m^{-2} day^{-1}; Urbini et al., 2020).~~.~~ Dense waters formed in the northern Adriatic can eventually flow towards the SAP, suggesting that the Southern Adriatic may act as a regional collector of carbon-enriched waters from upstream regions in addition to locally vertical transfer of CO_2 during convection events. Similarly, i~~I~~n the Gulf of Lion, Ulses et al. (2023) showed that the area functions as a net CO_2 sink on an annual scale, with an estimated carbon sequestration rate of approximately -1.29 mmol m^{-2} day^{-1} (estimated mean was -0.47 mol C m^{-2} year^{-1}). Here higher uptake is also linked to Atlantic inflow and spring primary production that lowers surface pCO$_2$ (Martellucci et al., 2025). Finally, comparable FCO$_2$ values could be also found between the SAd and the Central Mediterranean (Pecci et al., 2026) where estimates at the Lampedusa observatory, indicate a net CO_2 sink activity corresponding to −1.76 ± 0.11 mmol m^{-2} day^{-1} for a 1-year period (i.e., 2022).

4.3 ~~Estimated uncertainties~~Impact of different wind inputs in FCO$_2$ estimates

This section examines the influence of different wind products (in situ observations and ERA5 reanalysis), different temporal aggregations of the wind data (hourly, 6-hourly, and daily averages), and alternative gas transfer velocity parameterisations (Eq. (5), (6) and (7)) on the estimation of FCO$_2$. Flux estimates obtained using these different methodological choices are compared on both annual basis and for two extended seasonal periods representing the main hydrographic phases of the Southern Adriatic: the winter/convective period, from October to March, and the summer/post-convective period, from April to September. For each new estimates, the annual and seasonal averages were derived using the same approach of the nominal estimate (i.e., considering months with at least 14 valid daily observations). Annual and seasonal averages were then calculated from these monthly values. The resulting annual and seasonal FCO$_2$ estimates are summarized in Table 2. All configurations based on in situ observations consistently indicated a net annual uptake of atmospheric CO_2 by the Southern Adriatic, although the magnitude of the estimated flux varied depending on the methodological choices adopted (Table 2). Annual mean FCO$_2$ ranged from −0.90 to −3.92 mmol m^{-2} day^{-1}. The choice of the gas transfer velocity parameterisation had a larger influence on the annual flux estimate than the temporal aggregation of the wind data. While the results using k_W or k_N with any temporal aggregation produced comparable results, the use of $k_{W\&McG}$ produced higher results. For example, using the pair 6-hourly in situ wind speed and $k_{W\&McG}$ produced an annual uptake four times larger than estimates obtained with the pair 6-hourly in situ wind speed and k_W or k_N. The influence of wind temporal aggregation was generally limited for k_W or k_N but became more pronounced for $k_{W\&McG}$, which is inherently more sensitive to high wind speeds that can be smoothed out due to the daily aggregation of the data. At the seasonal scale, winter CO_2 uptake was consistently larger than summer outgassing regardless of the selected parameterisation or wind temporal aggregation. Winter mean FCO_2 ranged from −14.55 to −19.26 mmol m^{-2} day^{-1} using in situ winds, whereas summer values ranged between 8.75 and 13.96 mmol m^{-2} day^{-1}. The relative standard deviation of the summer estimates was, however, systematically higher than that of the winter period. This behaviour mainly reflects the inclusion of May in the summer period. As shown in Fig. 3b, May represents a transition month during which the Southern Adriatic shifts from winter sink conditions to summer source conditions. Although October also marked a seasonal transition, its influence on the winter mean was less pronounced because it was followed by several months characterized by persistent CO_2 uptake. In contrast, the summer period included only four months (from June to September) that consistently behave as a CO_2 source. These results suggested that the annual net CO_2 uptake in the Southern Adriatic is favoured not only by the higher winter CO_2 flux but also by the longer duration of the sink period relative to the source period. A different behaviour emerged when ERA5 wind data were used. Using ERA5 wind fields together with k_W and k_N parameterisations resulted in a weak annual CO_2 source, whereas the use of the nearest ERA5 grid point to the EMSO-E2M3A observatory instead of the spatial average resulted in a weak annual sink. This sign reversal highlighted the strong dependence of FCO_2 estimates on the representation of the local wind field. The difference was particularly evident during winter, when ERA5 spatially averaged winds produced CO_2 uptake estimates about 25–40% lower than those obtained using the nearest ERA5 grid point. This suggests that spatial averaging may smooth high wind events, which strongly influence k because of its nonlinear dependence on wind speed (Takahashi et al., 2002). A more detailed analysis on the performance of ERA5 wind in the region revealed that the largest discrepancy between ERA5 and in situ observations (Fig. S4 and Fig. S5, Supplementary Material) occurred during strong wind events (high Beaufort conditions).

Table 2. Air-sea CO_2 flux (mmol m^{-2} day^{-1}) in the Southern Adriatic calculated using different wind speed inputs from in situ observations (EMSO-E2M3A) and ERA5 reanalysis. ERA5 wind speed was tested both as a spatial mean over a 30 km radius around the observatory (ERA5 30 km spatial mean) and as the nearest grid point to EMSO-E2M3A (ERA5 single point). Different gas transfer velocity parametrisations (k_W, $k_{W\&McG}$, and k_N) and temporal aggregations of the wind data (hourly, 6-hourly, and daily averages) were compared. Flux estimates are reported as annual means and as seasonal means ± standard deviation for two extended periods: winter/convective period (October-March) and summer/post-convective period (April-September).

		EMSO-E2M3A			ERA5 30 km spatial mean	ERA5 single point
		Hourly	6-hours	Daily	6-hours	6-hours
Annual	k_W	-0.90	-0.97	-1.29	0.27	-1.11
	$k_{W\&McG}$	-3.92	-3.87	-3.26	-0.53	-2.81

	k_N	-0.97	-1.01	-0.90	0.49	-0.75
Winter (convective)	k_W	-14.56 ± 7.02	-15.90 ± 7.77	-14.55 ± 7.02	-8.91 ± 4.18	-12.27 ± 6.09
	$k_{W\&McG}$	-19.26 ± 9.85	-18.09 ± 9.12	-15.27 ± 7.55	-7.61 ± 3.56	-12.69 ± 6.53
	k_N	-15.91 ± 7.77	-15.51 ± 7.54	-14.56 ± 7.03	-9.27 ± 4.36	-12.37 ± 6.12
Summer (post-convective)	k_W	12.75 ± 13.73	13.97 ± 14.97	11.97 ± 13.13	9.45 ± 10.32	10.05 ± 10.75
	$k_{W\&McG}$	11.43 ± 13.67	10.36 ± 12.56	8.75 ± 10.69	6.55 ± 7.73	7.06 ± 8.16
	k_N	13.96 ± 14.97	13.47 ± 14.51	12.76 ± 13.73	10.26 ± 11	10.86 ± 11.43

The accuracy of the CO_2 flux estimates presented in this study was influenced by several systematic sources of uncertainty, arising from the type of data used to compute the two relevant parts of the W14 formula, i.e., the the gas transfer velocity k and the difference between pCO_{2sw} and pCO_{2atm} (ΔCO_2). To assess the source of uncertainty related to k, three different wind datasets were used to compute CO_2 flux other than the one used in Sec. 4.2. These considerations are particularly relevant given the presence of temporal gaps in the time series presented here. The first case (hereafter U1) considered the conversion applied to EMSO E2M3A wind speed data from 2 m to 10 m height (see Sec. 3.3). The second case (hereafter U2) accounted for the effect of a different temporal resolution considering a daily average of the wind data directly calculated from hourly observation without performing 6-hourly means. The use of 6-hourly wind speed averages is widely adopted as it smooths extreme values, reduces noise in buoy data, better represents the slow air–sea CO_2 exchange, and ensures consistency with model outputs. The third case (hereafter U3) used wind data from ERA5. Considering U3 is particularly relevant especially when in situ measurements are unavailable, and model-derived data must be integrated. Moreover, given that RD uses the same W14 formula and ERA5 wind data, the assessment of U3 can be used to help disentangling model errors that derive from the air-sea flux calculation (e.g., different wind products) from those derived from the ΔCO_2 discrepancies. Uncertainty in each of the three cases was quantified as the mean difference between fluxes calculated using the reference condition (10 m in situ wind speed averaged every 6 hours) and the alternative inputs (2 m height and 6 hours average in situ wind speed, for U1; daily average of 10 m height in situ wind speed, for U2; and 10 m height and 6 hours average ERA5 wind speed, for U3). For the ΔCO_2, the systematic uncertainty associated with the use of pCO_{2atm} derived using xCO_2 from Lampedusa site (Sec. 3.1) was considered. This latter, hereafter referred to as U4, was estimated by comparing winter fluxes calculated with the uncorrected pCO_{2atm} to those calculated after adding +2.67 µatm to the pCO_{2atm} time series (Sec. 3.1). All the uncertainties, except U4, were computed separately for two extended seasonal regimes: the summer/source period (from April to September) and the winter/sink period (from October to March). U4 was restricted to the winter period only as the offset of +2.67 µatm was computed considering winter months only (December to March, Sec. 3.1). A summary of the results is shown in Fig. 4.

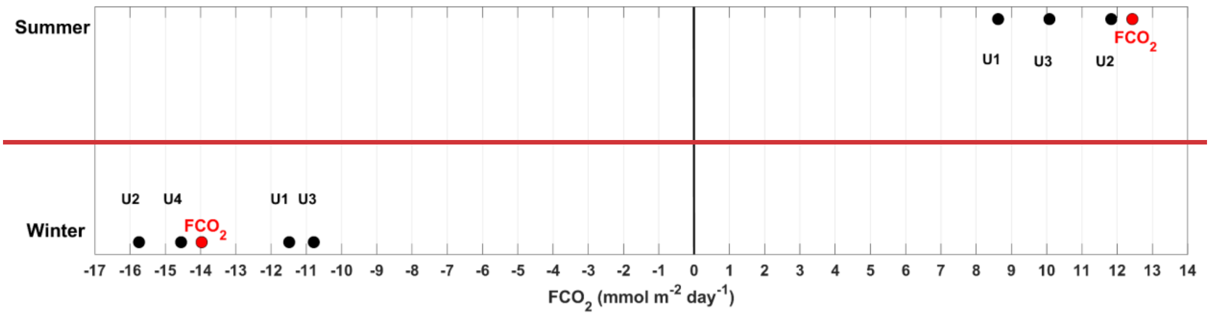

Figure 4. Summary of the different sources of uncertainties (U1, U2, U3, U4) considered in the study associated with the estimated FCO_2 (mmol m^{-2} day^{-1}) in the SAd (FCO_2 in red) in the period 2015-2024 calculated as described in Sec. 4.2. Winter includes the months from October to March and summer includes the months from April to September.

The different sources of uncertainty influenced FCO_2 estimates in different ways across seasons. The largest seasonal differences were observed for U1 and U3, whereas U2 showed lower variability between winter and summer. Among the three, U2 contributed the least to the overall uncertainty especially during summer, suggesting that the choice between using daily mean calculated from 6-hourly means or daily average calculated from hourly observations (without performing 6-hourly means) wind speed had only a minor effect on the final FCO_2 estimates. However, this choice appeared to have a higher influence during winter. The effect of using wind speed data at a lower height than the standard 10 m height (U1), as proposed in W14, has already been discussed (e.g., Griessbaum et al., 2010; Nickford et al., 2022; Nickford et al., 2024). The authors have shown that wind speed measured closer to the air-sea exchange interface could better represent the local forcing, particularly under conditions of high atmospheric stratification. Such measurements may also capture transient phenomena, including gusts and micro-turbulence, and could improve our understanding of the role of wave breaking and bubble-mediated transfer in modulating the CO_2 flux. While these aspects are beyond the scope of the present study, they highlighted the value of further investigations into near-surface wind dynamics for the estimation of FCO_2. U3 showed the largest differences with respect to FCO_2 estimated as described in Sec. 4.2, underscoring potential limitations in using ERA5 reanalysis data as a reliable regional proxy for local wind speed conditions. A more detailed analysis (Fig. S4, S5, Supplementary Material) revealed high differences between the wind speed measured at EMSO-E2M3A and ERA5 especially in high Beaufort scale wind (https://www.rmets.org/metmatters/beaufort-wind-scale). Given the quadratic dependence of *k* on wind speed, as a result, the choice of the wind speed field used is expected to lead to changes in FCO_2 as emphasized by Takahashi et al. (2002). Considering the uncertainty of the ΔCO_2 components, errors associated with corrected or not corrected pCO_{2atm} in the SAd were negligible. Finally, it is important to mention that in respect to ΔCO_2 the error related to the use of in situ sensor-based pCO_{2sw} as input for FCO_2 should also be computed. Sensor-based pCO_{2sw} not always met the manufacturer and the ICOS or SOCAT accuracies (Steinhoff et al., 2025). As shown in Dentico et al., (2025) the measured values by Pro-Oceanus membrane sensor can report higher (>10 µatm) differences with pCO_{2sw} calculated from discrete seawater samples. Here, it was not possible to compute a statistically robust measure of this uncertainty. This was due to the very low number of discrete seawater samples and the bias of their temporal distribution (Dentico et al., 2025). Most of the available pCO_{2sw} from discrete seawater samples were collected in October and not only failed to adequately represent the full seasonal cycle of CO_2. Additionally, October was the month that showed the transition from the positive to negative phases possibly emphasizing differences in FCO_2 calculation. While the random component of uncertainty can be quantified for pCO_{2sw} (e.g., using standard bootstrapping approaches based on the manufacturer-specified precision of the pCO_{2sw} sensor), the focus here was on the potentially systematic sources of uncertainty in the computation of FCO_2. This choice reflected the substantial effort involved in assembling multiple source dataset.

4.4. pCO_{2sw} and FCO_2: in situ data and model comparison

The in situ pCO_{2sw} and physical data proved to be a reliable asset for model validation, thus a comparison between the RD and AF CMEMS products for pCO_{2sw} and FCO_2 was computed. The comparison between daily pCO_{2sw} from CMEMS (Sect. 3.42) and pCO_{2sw} measured by the probe for a decade-long period highlighted a coherent temporal evolution (Fig. 5). A RMSE of 35.96 µatm and a significant correlation coefficient of 0.82 (*p value* < 0.01) between the two datasets was found. Nevertheless, during summer, model data were on average higher than pCO_{2sw} from the probe, with a mean difference between RD and the probe data of +34.22 µatm. The only exception was in 2022, when pCO_{2sw} from the probe was higher than CMEMS data (both RD and AF). As discussed in section 4.1 in 2022 a marine heatwave was detected in the region (Pirro et al., 2024). The strong difference in pCO_{2sw} between the probe and the model was likely driven by the combined effects of warming, enhanced stratification, and biogeochemical processes which are difficult to represent in current biogeochemical models. On the contrary, in winter RD data were on average lower than the probe, with a mean difference between the two datasets of -26.87 µatm. This discrepancy was mainly associated with can be explained by the increase in the pCO_{2sw} shown recorded by the probe data between late December and late February, which was not fully resolved by the model and was underestimated by that was not resolved by the model, which underestimated it by approximately 45 µatm. This mismatch may be partly attributed to the limited vertical resolution of the model and to the parameterization of vertical mixing processes, which may smooth or underestimate the upward transport of DIC to the surface during convection events (as discussed in Sect. 4.1). Finally, in autumn and spring the mean differences were smaller (+5.13 µatm and -16.12 µatm, respectively). By contrast, with lower intensity, the AF product was able to capture this increase (Fig. 5). Similarly to RD, also AF was not able to consistently reproduce the higher pCO_{2sw} values measured by the probe in summer 2022. Finally, in autumn and spring the mean differences were smaller (+5.13 µatm and -16.12 µatm, respectively).

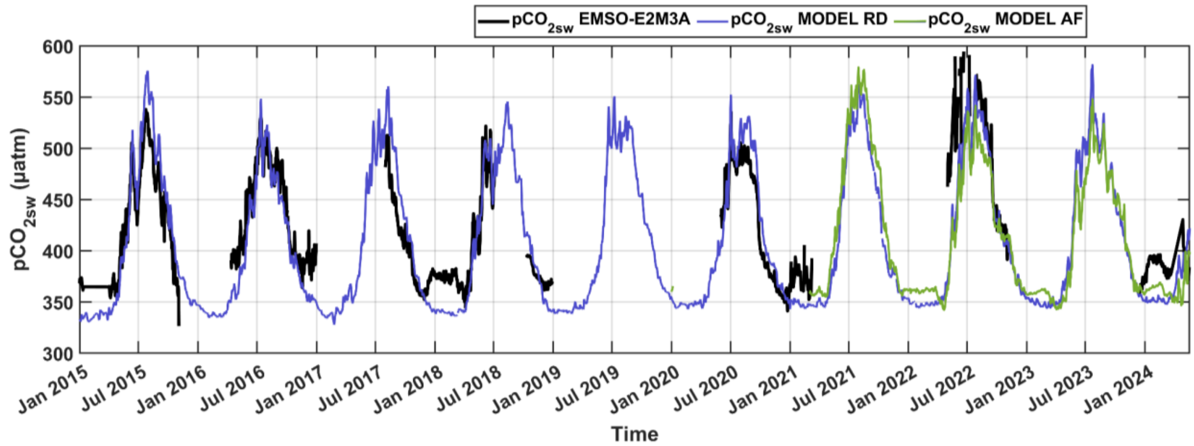

Figure 5. Time series of daily pCO_{2sw} (µatm) measured at the EMSO-E2M3A regional observatory in black, pCO_{2sw} (µatm) from the Mediterranean Sea Biogeochemistry Reanalysis (RD) in blue and the Mediterranean Sea Biogeochemistry Analysis and Forecast (AF) in green. RD data after July 2022 were integrated with the interim reanalysis.

The comparison between FCO_2 derived from in situ data and from the model is presented in Fig. 6. Both datasets consistently capture the two main seasonal phases of the region, with a source period during summer and a sink period during winter. However, notable differences in absolute values emerged, particularly in summer. A main factor in these differences was related to the pCO_{2sw} measurements as discussed in the previous section. Additionally, in both seasons, the different wind forcing used by the model (ERA5) could also be a contributing factor of the FCO_2 difference (see Sect. 4.3 and Fig. S5, Supplementary Material). On the contrary, the difference between model and in situ temperature and/or salinity was not considered a driving factor of the in situ and RD FCO_2 difference (Fig. S6, Supplementary Material). Nevertheless, an RMSE of 16.89 mmol m^{-2} day^{-1} with a correlation coefficient of 0.89 (p *value* < 0.01) was calculated between FCO_2 from RD and FCO_2 derived from observational data.

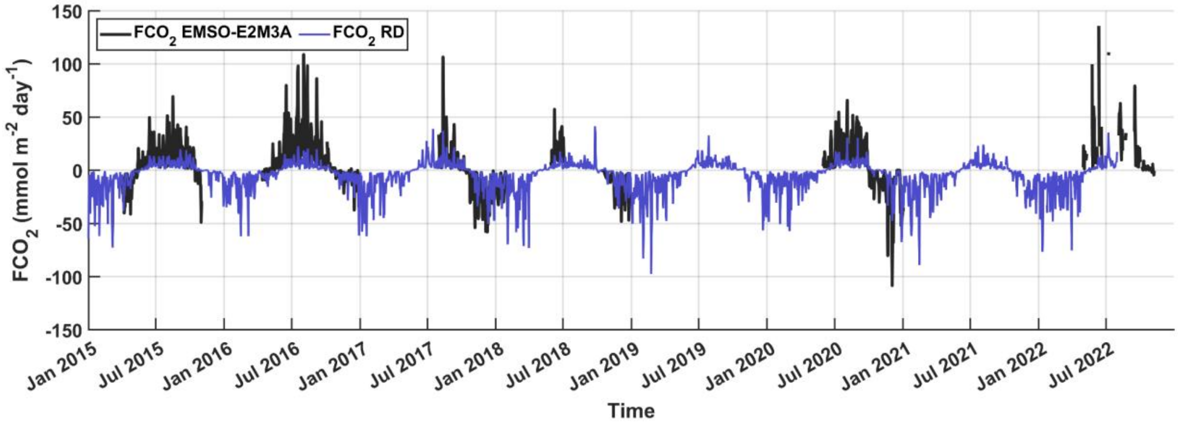

Figure 6. Time series of daily FCO_2 (mmol m^{-2} day^{-1}) calculated with in situ data measured at the EMSO-E2M3A and FCO_2 (mmol m^{-2} day^{-1}) from the Mediterranean Sea Biogeochemistry Reanalysis (RD) represented by the black and violet curves respectively. Model data after July 2022 were integrated with the interim reanalysis.

Considering the relatively good performance of the RD, and the temporal bias in the in situ FCO_2 time series (e.g., the winter periods were by far undersampled with respect to summer periods), it was used to clarify the role of the SAd as a source or sink of CO_2. The mean annual FCO_2 using exclusively CMEMS RD resulted in -4.33 mmol m^{-2} day^{-1}. The spatial distribution of the mean annual FCO_2 further highlighted that spatial differences in the basin existed (Figure 7). The strongest uptake is found in the central-deep part of the basin, where FCO_2 reaches values close to -5 mmol m^{-2} day^{-1} while weaker sink activity was shown particularly along the eastern part of the basin with values being between 0 and -2 mmol m^{-2} day^{-1} (Figure 7). Nevertheless, despite the spatial differences in the magnitude of the annual CO_2 fluxes, the overall basin-scale behaviour derived from the CMEMS reanalysis is consistent with the in situ observations. Although local fluxes vary across the basin, the EMSO-E2M3A can be considered a representative site for capturing the main carbon dynamics of the Southern Adriatic. Secondly, the use of the CMEMS RD product to compute the overall FCO_2 average filling the gaps of the in situ data was tested. A bias (B) ~~of~~ using the CMEMS RD was calculated as the difference between the mean flux over the entire period (2015-2024) and the mean flux considering only the days with observations being equal to -3.74 mmol m^{-2} day^{-1}. B was then added to the mean flux calculated with in situ observations, resulting in a mean annual flux of ~~-4.9 mmol m^{-2} day^{-1} and~~ -4.5 mmol m^{-2} day^{-1}~~, respectively for the two M1 and M2 methods~~.~~-~~, ~~-~~Even if these estimates should be considered with caution, they further confirm that the Southern Adriatic acted as a moderate carbon sink over the last decade.

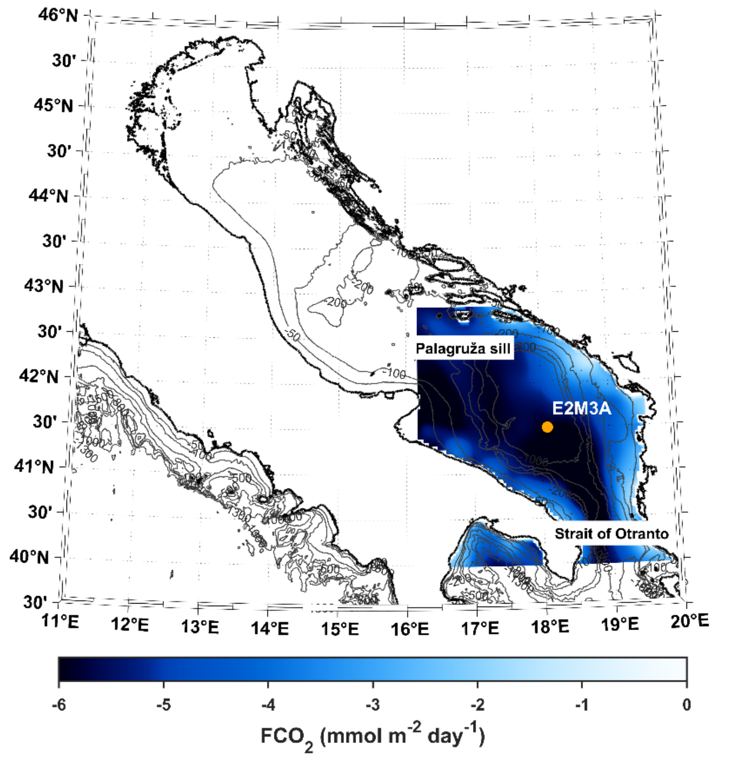

Figure 7. Spatial distribution of mean annual CO_2 flux (FCO_2, mmol m^{-2} day^{-1}) in the Southern Adriatic from CMEMS RD data. Negative values indicate a net uptake of atmospheric CO_2. Strongest FCO_2 were observed in the central deep basin, while weaker FCO_2 occurred along the eastern margins of the basin. Bathymetric contours are also shown. The EMSO-E2M3A mooring site, located in the central Southern Adriatic Pit, is indicated by the orange marker. The Palagruža Sill and the Strait of Otranto are included as geographical limits of the study area.

5. Conclusion

A time series of pCO_{2sw} and hydrography from autonomous sensors over the past 10 years were analyzed to characterize estimate pCO_{2sw} and carbon flux in the dense water formation site of the Ssouthern Adriatic Sea. The data were collected by several sensors deployed at the EMSO-E2M3A South Adriatic regional facility and ICOS ERIC observatory (nominal position 41.5053°N, 18.0806°E) which is located in the central and deepest part of the SAd, the SAP. Surface pCO_{2sw} dynamics were characterized by strong seasonal fluctuations, with a difference of 100 µatm between winter and summer. In winter, average pCO_{2sw} were around ~380 µatm, with marked increase especially during wintertime convection periods when CO_2-rich intermediate and deep water were upwelled to the surface. In summer, average values increased up to around 500 µatm driven by higher sea surface temperatures. The effect of biological processes was difficult to identify due to lower availability of data during post-convection/bloom periods. CO_2 fluxes were characterized by two distinct regimes of post-convection/summer CO_2 released to the atmosphere (mean summer month/source flux of +12.43 mmol m^{-2} day^{-1}) and convection/winter CO_2 ocean uptake (mean winter months/sink flux of -15.82 mmol m^{-2} day^{-1}). One of the key results of this study was to demonstrate that over the past decade the

SAd acted as a moderate carbon sink with mean annual FCO_2 values of about -0.97 mmol m^{-2} day^{-1}~~.~~ To evaluate the robustness of the flux estimates, additional FCO_2 calculations were performed using different wind products, temporal aggregations of the wind data, and gas transfer velocity parameterisations. All configurations based on in situ wind observations consistently indicated a net annual CO_2 uptake, despite differences in the magnitude of the estimated fluxes. Among the tested methodological choices, the gas transfer velocity parameterisation exerted the largest influence on the annual flux estimate, whereas the temporal aggregation of the wind data had a comparatively smaller effect. Conversely, the use of ERA5 wind products highlighted the importance of accurately representing the local wind field, as using a spatially averaged wind field instead of the nearest grid point to EMSO-E2M3A changed the annual CO_2 budget from a sink to a weak source. ~~Two different orders of aggregating the data for computing decadal averages were used due to the sampling irregularity. These calculations resulted in a mean sink flux of -1.15 mmol m^{-2} day^{-1} (M1) and -0.76 mmol m^{-2} day^{-1} (M2) in the period 2015-2024. Several sources of systematic uncertainty associated with the two most relevant parts of the flux formula, i.e., the gas transfer velocity (k) and ΔCO_2, were also quantified. For k, the selection of the wind forcing to be used in FCO_2 calculation is one of the primary sources of uncertainties. Particularly, the correction applied to convert in situ wind speed data from 2 m height to 10 m height and the use of ERA5 dataset as input variable for the calculation of FCO_2.~~ Thus, careful consideration must be given to ~~both~~ the wind product selected ~~and the height at which wind is measured or modelled, particularly in coastal areas or under high-wind conditions where gas exchange may be over- or underestimated (Nickford et al., 2024). Furthermore,~~ as many oceanic areas lack in situ wind observations, model-derived wind products (e.g., ERA5, CCMP) are ~~frequently~~ used instead~~used~~ (Nickford et al., 2024). ~~Assessing the reliability and limitations of these datasets is therefore critical for improving flux estimates in data-sparse regions. Regarding ΔCO_2, the use of pCO_{2atm} from another location appeared to have a minor influence on the final FCO_2. While in this study the focus was on systematic uncertainty, the pCO_{2sw} one was not estimated due to the lack of discrete seawater samples.~~ By proving to be an important asset for model validation, the pCO_{2sw} and hydrographic time series allowed to quantify existing specific discrepancies in the regional CMEMS model product such as a lack in winter pCO_{2sw} increase, and over/underestimation of the seasonal amplitude. Nevertheless, the integration of model and observational data further confirms that the SAd was a site of moderate atmospheric CO_2 sink in the last decade. The spatial distribution of modelled annual CO_2 flux further indicated that, despite regional heterogeneity and areas of weaker uptake, the Southern Adriatic overall behaved as a CO_2 sink on annual basis. This also supports the relevance of the EMSO-E2M3A observatory as a representative site for investigating the main carbon flux dynamics in the central part of the region.

The SAd, as many other regions in the Mediterranean Sea, is currently undergoing profound physical changes, including increasing sea surface temperature, rising salinity, and the potential intensification of extreme events. These trends are likely to affect convection intensity and timing, with potential consequences for carbon dynamics in the basin on a climatic scale. In this context, the long-term monitoring carried out in the region, by combining sustained in situ observations with modelling approaches, are necessary to fully understand the complex interplay between physical forcing, biogeochemical processes, and carbon dynamics in the context of climate change.

Data availability

The in situ data used in this study are freely accessible at the National Oceanographic Data Center (NODC) of the National Institute of Oceanography and Applied Geophysics (https://doi.org/10.13120/y2hw-1j63; Cardin et al., 2025b). Model data are also publicly available through the Copernicus Marine Service website following the links provided in the manuscript.

Team list:

Carlotta Dentico, Gianpiero Cossarini, Giuseppe Civitarese, Michele Giani, Angelo Rubino and Vanessa Cardin.

Author contribution:

CD: data curation, investigation, validation, writing (original draft), writing (review and editing), conceptualisation, formal analysis. GCos: investigation, writing (review and editing), conceptualisation. GCiv: investigation, writing (review and editing), conceptualisation. MG:investigation, writing (review and editing), conceptualisation. AR: investigation, writing (review and editing), conceptualisation. VC: funding acquisition, project administration, investigation, writing (review and editing), conceptualisation, supervision.

Competing interest:

The authors declare that they have no conflict of interest.

Acknowledgements:

This work benefited from access to the E2M3A South Adriatic Regional Facility, an EMSO-IT/ICOS-IT site operated by OGS. This study has been conducted using E.U. Copernicus Marine Service Information. The authors are very grateful to the OGS technical and biogeochemical teams, as well as the CNR-ISP for their essential contributions and continued efforts in operating and maintaining the EMSO/ICOS-E2M3A regional facility. The authors also acknowledge ChatGPT creators as it was used to improve the English writing in some parts of this manuscript.

Financial support: The dataset used and the related activities were partially funded by the EMSO Italian Joint Research Unit, OGS, and the EU Next Generation EU programme (Mission 4, Component 2, Investment 3.1: “Fund for the realisation of an integrated system of research and innovation infrastructures") under Project IR0000032 – ITINERIS (Italian Integrated Environmental Research Infrastructures System). Additional support for pCO_2 instruments data acquisition and calibration was also provided by ICOS.

References

Álvarez, M., Sanleón-Bartolomé, H., Tanhua, T., Mintrop, L., Luchetta, A., Cantoni, C., Schroeder, K., and Civitarese, G.: The CO_2 system in the Mediterranean Sea: a basin wide perspective, Ocean Sci., 10, 69–92, https://doi.org/10.5194/os-10-69-2014, 2014.

Alvarez, M., Catala, S.T., Civitarese, G., Coppola, L., Hassoun, A., Ibello, V., Lazzari, P., Lefevre, D., Macias, D., Santinelli, C., and Ulse, C.: Mediterranean Sea general biogeochem istry, in: Oceanography of the Mediterranean Sea, edited by: Schroeder, K., and Chiggiato, J., Elsevier, Amsterdam, 387–451, https://doi.org/10.1016/B978-0-12-823692-5.00004-2, 2023.

Álvarez, M., García-Ibáñez, M. I., Lange, N., Kozyr, A.,Velo, A., Tanhua, T., Civitarese, G., Cantoni, C., Belgacem, M., Schroeder, K., Acerbi, R., Coppola, L., Wagener, T., Fajar, N. M., Flecha, S., Giani, M., Giannoudi, L., Guallart, E.F., El Rahman Hassoun, A., Huertas, E. I., Ibello, V., Keraghel, M. A., Louanchi, F., Luchetta, A., Pérez, F. F., Schirnick, C., Souvermezoglou, E., Urbini, L., Vidal, M., and Ziveri, P.: CARIMED (CARbon, tracers, and ancillary data In the MEDiterranean Sea): a ship-based data synthesis product – overview and quality control procedures. Earth System Science Data , 18, 4915–4941, https://doi.org/10.5194/essd-18-4915-2026, 2026.

Amitai, Y., Ashkenazy, Y., and Gildor, H.: The Effect of the Source of Deep Water in the Eastern Mediterranean on Western Mediterranean Intermediate and Deep Water, Front. Mar. Sci., 7, 615975, https://doi.org/10.3389/fmars.2020.615975, 2021.

Amorim, F. L. L., Le Meur, J., Wirth, A., and Cardin, V.: Tipping of the double-diffusive regime in the southern Adriatic Pit in 2017 in connection with record high-salinity values, Ocean Sci., 20, 463–474, https://doi.org/10.5194/os-20-463-2024, 2024.

~~Atlas, R., Hoffman, R. N., Ardizzone, J., Leidner, S. M., Jusem, J. C., Smith, D. K., and Gombos, D.: A Cross-calibrated, Multiplatform Ocean Surface Wind Velocity Product for Meteorological and Oceanographic Applications, Bull. Amer. Meteor. Soc., 92, 157–174, https://doi.org/10.1175/2010BAMS2946.1, 2011.~~

Agustí-Panareda, A., Barré, J., Massart, S., Inness, A., Aben, I., Ades, M., Baier, B. C., Balsamo, G., Borsdorff, T., Bousserez, N., Boussetta, S., Buchwitz, M., Cantarello, L., Crevoisier, C., Engelen, R., Eskes, H., Flemming, J., Garrigues, S., Hasekamp, O., Huijnen, V., Jones, L., Kipling, Z., Langerock, B., McNorton, J., Meilhac, N., Noël, S., Parrington, M., Peuch, V.-H., Ramonet, M., Razinger, M., Reuter, M., Ribas, R., Suttie, M., Sweeney, C., Tarniewicz, J., and Wu, L.: Technical note: The CAMS greenhouse gas reanalysis from 2003 to 2020, Atmos. Chem. Phys., 23, 3829–3859, https://doi.org/10.5194/acp-23-3829-2023, 2023.

Bakker, D. C., Alin, S. R., Bates, N. R., Becker, M., Feely, R. A., and Gritzalis, T.: ~~(2023)~~. SOCAT version 2023– An alarming decline in the ocean CO_2 observing capacity, 2023.~~.~~

Bakker, D. C. E., Alin, S. R., Bates, N., Ehmen, T., Gkritzalis, T., Jones, S. D., Kamb, L., Kozyr, A., Lauvset, S. K., Macovei, V. A., Metzl, N., Nakaoka, S., O'Brien, K. M., Olsen, A., Pierrot, D., Poelmans, S., Steinhoff, T., Sutton, A. J., Sweeney, C., Takao, S., Telszewski, M., Theetaert, H., Tilbrook, B., Wada, C., Wanninkhof, R., Akl, J., Aramaki, T., Arbilla, L. A., Avila, R., Baier, B., Barbero, L., Battisti, R., Beatty, C. M., Becker, H., Benoit-Cattin, A., Berghoff, C. F., Bittig, H. C., Bonin, J. A., Bozzano, R., Burger, E. F., Cai, W.,; Cantoni, C., Castelli, G., Castro Á. A., Chambers, D. P., Chierici, M., Cronin, M., Cubiella, Á. H., Curbelo-Hernández, D., Curless, S., Czyz, C., Diverrès, D., Dougherty, S., Enochs, I. C., Enright, M. P., Enyo, K., Evans, W., Feely, R. A., Flohr, A., Fragiacomo, E., Frangoulis, C., Fransson, A., Gehrung, M., Glockzin, M., González, A. G., González-Dávila, M., González-Santana, D., Hales, B., Hamnca, S., Hartman, S. E., Hermes, R., Herndon, J., Hoppema, M., Howard, E., Huertas, I. E., Kerr, R., Kristensen, T., Landschützer, P., Lee, C. M., Lee, H., Lefèvre, N., Leseurre, C., Lo Monaco, C., Luchetta, A., Maenner Jones, S., Manalang, D., McAuliffe, Anna M., Mdokwana, B., Monacci, N. M., Monteiro, P. M. S., Morell, J. M., Munro, D. R., Neill, C., Newberger, T., Nickford, S. E., Nilsson, E., Noakes, S., Noh, J-H., Noisel, C., O'Brien, C., Olivier, L., Omar, A. M., Orselli, I., Padín, X. A., Pena González, L. D., Pensieri, S., Prytherch, J., Rehder, G., Rutgersson, A., Sabine, C. L., Sallée, J-B., Sanders, R., Santana-Casiano, J. M., Sarpe, D., Schirnick, C., Schlitzer, R., Shadwick, E. H., Skjelvan, I., T'Jampens, M., Tamsitt, V., Toledo Aboy, A. E., Tovar-Sánchez, A., Tsanwani, M., van de Velde, S., van Ooijen, E., Vandemark, D., Veccia, M. H., Voynova, Y. G., Williams, N. L., Xu, Y-Y.. Surface Ocean CO_2 Atlas Database Version 2026 (SOCATv2026) (NCEI Accession 0315110). NOAA National Centers for Environmental Information. [dataset], https://doi.org/10.25921/8dba-fr90, 2026.

Benson, B. B. and Krause, D.: The concentration and isotopic fractionation of oxygen dissolved in freshwater and seawater in equilibrium with the atmosphere1, Limnology & Oceanography, 29, 620–632, https://doi.org/10.4319/lo.1984.29.3.0620, 1984.

~~Bignami, F., Salusti, E., and Schiarini, S.: Observations on a bottom vein of dense water in the southern Adriatic and Ionian seas, J. Geophys. Res., 95, 7249–7259, https://doi.org/10.1029/JC095iC05p07249, 1990.~~

Cantoni, C., Luchetta, A., Chiggiato, J., Cozzi, S., Schroeder, K., and Langone, L.: Dense water flow and carbonate system in the southern Adriatic: A focus on the 2012 event, Marine Geology, 375, 15–27, https://doi.org/10.1016/j.margeo.2015.08.013, 2016.

Cantoni, C., De Vittor, C., Faganeli, J., Giani, M., Kovač, N., Malej, A., Ogrinc, N., Tamše, S., and Turk, V.: Carbonate system and acidification of the Adriatic Sea, Marine Chemistry, 267, 104462, https://doi.org/10.1016/j.marchem.2024.104462, 2024.

Cardin, V., Bensi, M., and Pacciaroni, M.: Variability of water mass properties in the last two decades in the South Adriatic Sea with emphasis on the period 2006–2009, Continental Shelf Research, 31, 951–965, https://doi.org/10.1016/j.csr.2011.03.002, 2011.

Cardin, V., Le Meur, J., Ursella, L., Dentico, C., Siena, G., Mansutti, P., Brunetti, F., and Partescano, E.: EMSOE2M3A-Water-Column-time-series-South-Adriatic, OGS [data set], https://doi.org/10.13120/ZE9Q-3E51, 2025a.

~~Cardin, V., Le Meur, J., Ursella, L., Dentico, C., Siena, G., Mansutti, P., Brunetti, F., and Partescano, E.: EMSO-E2M3A-B-Surface-time-series-South-Adriatic [dataset], https://doi.org/10.13120/y2hw-1j63, 2025a.~~

Cardin, V., Dentico, C., Brunetti, F., Bubbi, A., Chiaruttini, L., Civitarese, G., Comici, C., Corbo, A., Gerin, R., Giani, M., Kuchler, S., Le Meur, J., Mansutti, P., Savonitto, G. and Siena, G.: EMSO-E2M3A-B-Surface-time-series-South-Adriatic [dataset], https://doi.org/10.13120/y2hw-1j63, 2025b.

Catalano, G., Azzaro, M., Bastianini, M., Bellucci, L. G., Bernardi Aubry, F., Bianchi, F., Burca, M., Cantoni, C., Caruso, G., Casotti, R., Cozzi, S., Del Negro, P., Fonda Umani, S., Giani, M., Giuliani, S., Kovacevic, V., La Ferla, R., Langone, L., Luchetta, A., Monticelli, L. S., Piacentino, S., Pugnetti, A., Ravaioli, M., Socal, G., Spagnoli, F., and Ursella, L.: The carbon budget in the northern Adriatic Sea, a winter case study, JGR Biogeosciences, 119, 1399–1417, https://doi.org/10.1002/2013JG002559, 2014.

Cerino, F., Bernardi Aubry, F., Coppola, J., La Ferla, R., Maimone, G., Socal, G., and Totti, C.: Spatial and temporal variability of pico-, nano- and microphytoplankton in the offshore waters of the southern Adriatic Sea (Mediterranean Sea), Continental Shelf Research, 44, 94–105, https://doi.org/10.1016/j.csr.2011.06.006, 2012.

Chiggiato, J., Bergamasco, A., Borghini, M., Falcieri, F. M., Falco, P., Langone, L., Miserocchi, S., Russo, A., and Schroeder, K.: Dense-water bottom currents in the Southern Adriatic Sea in spring 2012, Marine Geology, 375, 134–145, https://doi.org/10.1016/j.margeo.2015.09.005, 2016.

Civitarese, G., Gačić, M., Lipizer, M., and Eusebi Borzelli, G. L.: On the impact of the Bimodal Oscillating System (BiOS) on the biogeochemistry and biology of the Adriatic and Ionian Seas (Eastern Mediterranean), Biogeosciences, 7, 3987–3997, https://doi.org/10.5194/bg-7-3987-2010, 2010.

Civitarese, G., Gačić, M., Batistić, M., Bensi, M., Cardin, V., Dulčić, J., Garić, R., and Menna, M.: The BiOS mechanism: History, theory, implications, Progress in Oceanography, 216, 103056, https://doi.org/10.1016/j.pocean.2023.103056, 2023.

Coppola, L., Boutin, J., Gattuso, J., Lefevre, D., and Metzl, N.: The Carbonate System in the Ligurian Sea, in: The Mediterranean Sea in the Era of Global Change 1, edited by: Migon, C., Nival, P., and Sciandra, A., Wiley, 79–103, https://doi.org/10.1002/9781119706960.ch4, 2020.

Cossarini, G., Feudale, L., Teruzzi, A., Bolzon, G., Coidessa, G., Solidoro, C., Di Biagio, V., Amadio, C., Lazzari, P., Brosich, A., and Salon, S.: High-Resolution Reanalysis of the Mediterranean Sea Biogeochemistry (1999–2019), Front. Mar. Sci., 8, 741486, https://doi.org/10.3389/fmars.2021.741486, 2021.

Dentico, C., Rubino, A., Civitarese, G., Giani, M., Siena, G., Kuchler, S., Le Meur, J., Corbo, A., and Cardin, V.: Surface pCO_2 and hydrography in the dense water formation area of the southern Adriatic, Earth Syst. Sci. Data, 18, 2119–2131, https://doi.org/10.5194/essd-18-2119-2026, 2026.

Doney, S. C., Fabry, V. J., Feely, R. A., and Kleypas, J. A.: Ocean Acidification: The Other CO_2 Problem, Annu. Rev. Mar. Sci., 1, 169–192, https://doi.org/10.1146/annurev.marine.010908.163834, 2009.

Escudier, R., Clementi, E., Cipollone, A., Pistoia, J., Drudi, M., Grandi, A., Lyubartsev, V., Lecci, R., Aydogdu, A., Delrosso, D., Omar, M., Masina, S., Coppini, G., and Pinardi, N.: A High Resolution Reanalysis for the Mediterranean Sea, Front. Earth Sci., 9, 702285, https://doi.org/10.3389/feart.2021.702285, 2021.

Fay, A. R., Munro, D. R., McKinley, G. A., Pierrot, D., Sutherland, S. C., Sweeney, C., and Wanninkhof, R.: Updated climatological mean ΔfCO_2 and net sea–air CO_2 flux over the global open ocean regions, Earth Syst. Sci. Data, 16, 2123–2139, https://doi.org/10.5194/essd-16-2123-2024, 2024.

Fourrier, M., Coppola, L., D'Ortenzio, F., Migon, C., and Gattuso, J.: Impact of Intermittent Convection in the Northwestern Mediterranean Sea on Oxygen Content, Nutrients, and the Carbonate System, JGR Oceans, 127, e2022JC018615, https://doi.org/10.1029/2022JC018615, 2022.

Frangoulis, C., Stamataki, N., Pettas, M., Michelinakis, S., King, A. L., Giannoudi, L., Tsiaras, K., Christodoulaki, S., Seppälä, J., Thyssen, M., Borges, A. V., and Krasakopoulou, E.: A carbonate system time series in the Eastern Mediterranean Sea. Two years of high-frequency in-situ observations and remote sensing, Front. Mar. Sci., 11, 1348161, https://doi.org/10.3389/fmars.2024.1348161, 2024.

Friedlingstein, P., O'Sullivan, M., Jones, M. W., Andrew, R. M., Hauck, J., Landschützer, P., Le Quéré, C., Li, H., Luijkx, I. T., Olsen, A., Peters, G. P., Peters, W., Pongratz, J., Schwingshackl, C., Sitch, S., Canadell, J. G., Ciais, P., Jackson, R. B., Alin, S. R., Arneth, A., Arora, V., Bates, N. R., Becker, M., Bellouin, N., Berghoff, C. F., Bittig, H. C., Bopp, L., Cadule, P., Campbell, K., Chamberlain, M. A., Chandra, N., Chevallier, F., Chini, L. P., Colligan, T., Decayeux, J., Djeutchouang, L. M., Dou, X., Duran Rojas, C., Enyo, K., Evans, W., Fay, A. R., Feely, R. A., Ford, D. J., Foster, A., Gasser, T., Gehlen, M., Gkritzalis, T., Grassi, G., Gregor, L., Gruber, N., Gürses, Ö., Harris, I., Hefner, M., Heinke, J., Hurtt, G. C., Iida, Y., Ilyina, T., Jacobson, A. R., Jain, A. K., Jarníková, T., Jersild, A., Jiang, F., Jin, Z., Kato, E., Keeling, R. F., Klein Goldewijk, K., Knauer, J., Korsbakken, J. I., Lan, X., Lauvset, S. K., Lefèvre, N., Liu, Z., Liu, J., Ma, L., Maksyutov, S., Marland, G., Mayot, N., McGuire, P. C., Metzl, N., Monacci, N. M., Morgan, E. J., Nakaoka, S.-I., Neill, C., Niwa, Y., Nützel, T., Olivier, L., Ono, T., Palmer, P. I., Pierrot, D., Qin, Z., Resplandy, L., Roobaert, A., Rosan, T. M., Rödenbeck, C., Schwinger, J., Smallman, T. L., Smith, S. M., Sospedra-Alfonso, R., Steinhoff, T., et al.: Global Carbon Budget 2024, Earth Syst. Sci. Data, 17, 965–1039, https://doi.org/10.5194/essd-17-965-2025, 2025.

Gattuso, J-P, and Hansson L. (Eds). Ocean acidification. Oxford university press, 2011

Gačić, M., Civitarese, G., Miserocchi, S., Cardin, V., Crise, A., and Mauri, E.: The open-ocean convection in the Southern Adriatic: a controlling mechanism of the spring phytoplankton bloom, Continental Shelf Research, 22, 1897–1908, https://doi.org/10.1016/S0278-4343(02)00050-X, 2002.

Gačić, M., Borzelli, G. L. E., Civitarese, G., Cardin, V., and Yari, S.: Can internal processes sustain reversals of the ocean upper circulation? The Ionian Sea example, Geophysical Research Letters, 37, 2010GL043216, https://doi.org/10.1029/2010GL043216, 2010.

Garcia, H. E. and Gordon, L. I.: Oxygen solubility in seawater: Better fitting equations, Limnol. Oceanogr., 37, 1307–1312, https://doi.org/10.4319/lo.1992.37.6.1307, 1992.

García-Ibáñez, M. I., Guallart, E. F., Lucas, A., Pascual, J., Gasol, J. M., Marrasé, C., Calvo, E., and Pelejero, C.: Two new coastal time-series of seawater carbonate system variables in the NW Mediterranean Sea: rates and mechanisms controlling pH changes, Front. Mar. Sci., 11, 1348133, https://doi.org/10.3389/fmars.2024.1348133, 2024.

Giani, M., Ogrinc, N., Tamše, S., and Cozzi, S.: Elevated River Inputs of the Total Alkalinity and Dissolved Inorganic Carbon in the Northern Adriatic Sea, Water, 15, 894, https://doi.org/10.3390/w15050894, 2023.

Griessbaum, F., Moat, B. I., Narita, Y., Yelland, M. J., Klemm, O., and Uematsu, M.: Uncertainties in wind speed dependent CO_2 transfer velocities due to airflow distortion at anemometer sites on ships, Atmos. Chem. Phys., 10, 5123–5133, https://doi.org/10.5194/acp-10-5123-2010, 2010.

Gruber, N., Bakker, D. C. E., DeVries, T., Gregor, L., Hauck, J., Landschützer, P., McKinley, G. A., and Müller, J. D.: Trends and variability in the ocean carbon sink, Nat Rev Earth Environ, 4, 119–134, https://doi.org/10.1038/s43017-022-00381-x, 2023.

Gulev, S. K., Thorne, P. W., Ahn, J., Dentener, F. J., Domingues, C. M., Gerland, S., Gong, D., Kaufman, D. S., Nnamchi, H. C., Quaas, J., Rivera, J. A., Sathyendranath, S., Smith, S. L., Trewin, B., von Schuckmann, K., and Vose, R. S.: Changing State of the Climate System, in: Climate Change 2021: The Physical Science Basis. Contribution of Working Group I to the Sixth Assessment Report of the Intergovernmental Panel on Climate Change, edited by: Masson-Delmotte, V., Zhai, P., Pirani, A., Connors, S. L., Péan, C., Berger, S., Caud, N., Chen, Y., Goldfarb, L., Gomis, M. I., Huang, M., Leitzell, K., Lonnoy, E., Matthews, J. B. R., Maycock, T. K., Waterfield, T., Yelekçi, O., Yu, R., and Zhou, B., Cambridge University Press, Cambridge, United Kingdom and New York, NY, USA, 287–422, https://doi.org/10.1017/9781009157896.004, 2021.

Hassoun, A. E. R., Fakhri, M., Raad, N., Abboud-Abi Saab, M., Gemayel, E., and De Carlo, E. H.: The carbonate system of the Eastern-most Mediterranean Sea, Levantine Sub-basin: Variations and drivers, Deep Sea Research Part II: Topical Studies in Oceanography, 164, 54–73, https://doi.org/10.1016/j.dsr2.2019.03.008, 2019.

Hassoun, A. E. R., Bantelman, A., Canu, D., Comeau, S., Galdies, C., Gattuso, J.-P., Giani, M., Grelaud, M., Hendriks, I. E., Ibello, V., Idrissi, M., Krasakopoulou, E., Shaltout, N., Solidoro, C., Swarzenski, P. W., and Ziveri, P.: Ocean acidification research in the Mediterranean Sea: Status, trends and next steps, Front. Mar. Sci., 9, 892670, https://doi.org/10.3389/fmars.2022.892670, 2022.

Hersbach, H., Bell, B., Berrisford, P., Biavati, G., Horányi, A., Muñoz Sabater, J., Nicolas, J., Peubey, C., Radu, R., Rozum, I., Schepers, D., Simmons, A., Soci, C., Dee, D., Thépaut, J-N.: ERA5 hourly data on single levels from 1940 to present. Copernicus Climate Change Service (C3S) Climate Data Store (CDS), [dataset], https//doi.org/10.24381/cds.adbb2d47, 2023.

Ilyina, T., Zeebe, R. E., Maier-Reimer, E., and Heinze, C.: Early detection of ocean acidification effects on marine calcification, Global Biogeochemical Cycles, 23, 2008GB003278, https://doi.org/10.1029/2008GB003278, 2009.

Ingrosso, G., Giani, M., Comici, C., Kralj, M., Piacentino, S., De Vittor, C., and Del Negro, P.: Drivers of the carbonate system seasonal variations in a Mediterranean gulf, Estuarine, Coastal and Shelf Science, 168, 58–70, https://doi.org/10.1016/j.ecss.2015.11.001, 2016.

Ingrosso, G., Bensi, M., Cardin, V., and Giani, M.: Anthropogenic CO2 in a dense water formation area of the Mediterranean Sea, Deep Sea Research Part I: Oceanographic Research Papers, 123, 118–128, https://doi.org/10.1016/j.dsr.2017.04.004, 2017.

Intergovernmental Panel On Climate Change (~~Ipcc~~IPCC): Climate Change 2021 – The Physical Science Basis: Working Group I Contribution to the Sixth Assessment Report of the Intergovernmental Panel on Climate Change, 1st ed., Cambridge University Press, https://doi.org/10.1017/9781009157896, 2023.

Kapsenberg, L., Alliouane, S., Gazeau, F., Mousseau, L., and Gattuso, J.-P.: Coastal ocean acidification and increasing total alkalinity in the northwestern Mediterranean Sea, Ocean Sci., 13, 411–426, https://doi.org/10.5194/os-13-411-2017, 2017.

Lan, X., Tans, P. and K.W. Thoning: Trends in globally-averaged CO2 determined from NOAA Global Monitoring Laboratory measurements. Version Friday, 05-Dec-2025 11:36:40 MST: https://gml.noaa.gov/ccgg/trends/global.html, last access: 16 December 2025.

Laruelle, G. G., Cai, W.-J., Hu, X., Gruber, N., Mackenzie, F. T., and Regnier, P.: Continental shelves as a variable but increasing global sink for atmospheric carbon dioxide, Nat Commun, 9, 454, https://doi.org/10.1038/s41467-017-02738-z, 2018.

Le Meur, J., Wirth, A., Paladini De Mendoza, F., Miserocchi, S., and Cardin, V.: Intermittent supply of dense water to the deep South Adriatic Pit: an observational study, Front. Mar. Sci., 12, 1516780, https://doi.org/10.3389/fmars.2025.1516780, 2025.

Le Traon, P. Y., Reppucci, A., Alvarez Fanjul, E., Aouf, L., Behrens, A., Belmonte, M., Bentamy, A., Bertino, L., Brando, V. E., Kreiner, M. B., Benkiran, M., Carval, T., Ciliberti, S. A., Claustre, H., Clementi, E., Coppini, G., Cossarini, G., De Alfonso Alonso-Muñoyerro, M., Delamarche, A., Dibarboure, G., Dinessen, F., Drevillon, M., Drillet, Y., Faugere, Y., Fernández, V., Fleming, A., Garcia-Hermosa, M. I., Sotillo, M. G., Garric, G., Gasparin, F., Giordan, C., Gehlen, M., Gregoire, M. L., Guinehut, S., Hamon, M., Harris, C., Hernandez, F., Hinkler, J. B., Hoyer, J., Karvonen, J., Kay, S., King, R., Lavergne, T., Lemieux-Dudon, B., Lima, L., Mao, C., Martin, M. J., Masina, S., Melet, A., Buongiorno Nardelli, B., Nolan, G., Pascual, A., Pistoia, J., Palazov, A., Piolle, J. F., Pujol, M. I., Pequignet, A. C., Peneva, E., Pérez Gómez, B., Petit De La Villeon, L., Pinardi, N., Pisano, A., Pouliquen, S., Reid, R., Remy, E., Santoleri, R., Siddorn, J., She, J., Staneva, J., Stoffelen, A., Tonani, M., Vandenbulcke, L., Von Schuckmann, K., Volpe, G., Wettre, C., and Zacharioudaki, A.: From Observation to Information and Users: The Copernicus Marine Service Perspective, Front. Mar. Sci., 6, 234, https://doi.org/10.3389/fmars.2019.00234, 2019.

Lee, K., Sabine, C. L., Tanhua, T., Kim, T.-W., Feely, R. A., and Kim, H.-C.: Roles of marginal seas in absorbing and storing fossil fuel CO2, Energy Environ. Sci., 4, 1133, https://doi.org/10.1039/c0ee00663g, 2011.

Lohbeck, K. T., Riebesell, U., and Reusch, T. B. H.: Adaptive evolution of a key phytoplankton species to ocean acidification, Nature Geosci, 5, 346–351, https://doi.org/10.1038/ngeo1441, 2012.

~~Malanotte-Rizzoli, P.: The Northern Adriatic Sea as a Prototype of Convection and Water Mass Formation on the Continental Shelf, in: Elsevier Oceanography Series, vol. 57, Elsevier, 229–239, https://doi.org/10.1016/S0422-9894(08)70070-9, 1991.~~

Mantziafou, A. and Lascaratos, A.: An eddy resolving numerical study of the general circulation and deep-water formation in the Adriatic Sea, Deep Sea Research Part I: Oceanographic Research Papers, 51, 921–952, https://doi.org/10.1016/j.dsr.2004.03.006, 2004.

Martellucci, R., Giani, M., Mauri, E., Coppola, L., Paulsen, M., Fourrier, M., Pensieri, S., Cardin, V., Dentico, C., Bozzano, R., Cantoni, C., Lucchetta, A., Izquierdo, A., Bruno, M., and Skjelvan, I.: CO_2 and hydrography acquired by autonomous surface vehicles from the Atlantic Ocean to the Mediterranean Sea: data correction and validation, Earth Syst. Sci. Data, 16, 5333–5356, https://doi.org/10.5194/essd-16-5333-2024, 2024a.

Martellucci, R., Menna, M., Mauri, E., Pirro, A., Gerin, R., Paladini De Mendoza, F., Garić, R., Batistić, M., Di Biagio, V., Giordano, P., Langone, L., Miserocchi, S., Gallo, A., Notarstefano, G., Savonitto, G., Bussani, A., Pacciaroni, M., Zuppelli, P., and Poulain, P.-M.: Recent changes of the dissolved oxygen distribution in the deep convection cell of the southern Adriatic Sea, Journal of Marine Systems, 245, 103988, https://doi.org/10.1016/j.jmarsys.2024.103988, 2024b.

Martellucci, R., Dentico, C., Coppola, L., Skjelvan, I., Giani, M., Pensieri, S., Cantoni, C., Cardin, V., Fourrier, M., Bozzano, R., Paulsen, M., and Mauri, E.: Air-sea CO2 exchange in the Eastern Atlantic and the Mediterranean Sea based on autonomous surface measurements, Front. Mar. Sci., 12, 1633617, https://doi.org/10.3389/fmars.2025.1633617, 2025.

Marullo, S., Pitarch, J., Bellacicco, M., Sarra, A. G. D., Meloni, D., Monteleone, F., Sferlazzo, D., Artale, V., and Santoleri, R.: Air–Sea Interaction in the Central Mediterranean Sea: Assessment of Reanalysis and Satellite Observations, Remote Sensing, 13, 2188, https://doi.org/10.3390/rs13112188, 2021.

Matek, A., Mucko, M., Casotti, R., Trano, A. C., Achterberg, E. P., Mihanović, H., Čižmek, H., Čolić, B., Cuculić, V., and Ljubešić, Z.: Phytoplankton Diversity and Co-Dependency in a Stratified Oligotrophic Ecosystem in the South Adriatic Sea, Water, 15, 2299, https://doi.org/10.3390/w15122299, 2023.

Menna, M., Martellucci, R., Notarstefano, G., Mauri, E., Gerin, R., Pacciaroni, M., Bussani, A., Pirro, A., Poulain, P-M.: Record-breaking high salinity in the South Adriatic Pit in 2020, in: Copernicus Ocean State Report, issue 6. Journal of Operational Oceanography, 15(sup1), 1–220. https://doi.org/10.1080/1755876X.2022.2095169, 2022.

Merlivat, L., Boutin, J., Antoine, D., Beaumont, L., Golbol, M., and Vellucci, V.: Increase of dissolved inorganic carbon and decrease in pH in near-surface waters in the Mediterranean Sea during the past two decades, Biogeosciences, 15, 5653–5662, https://doi.org/10.5194/bg-15-5653-2018, 2018.

Matek, A., Mucko, M., Casotti, R., Trano, A. C., Achterberg, E. P., Mihanović, H., Čižmek, H., Čolić, B., Cuculić, V., and Ljubešić, Z.: Phytoplankton Diversity and Co-Dependency in a Stratified Oligotrophic Ecosystem in the South Adriatic Sea, Water, 15, 2299, https://doi.org/10.3390/w15122299, 2023.

Meyer, J. and Riebesell, U.: Reviews and Syntheses: Responses of coccolithophores to ocean acidification: a meta-analysis, Biogeosciences, 12, 1671–1682, https://doi.org/10.5194/bg-12-1671-2015, 2015.

Metzl, N., Fin, J., Lo Monaco, C., Mignon, C., Alliouane, S., Bombled, B., Boutin, J., Bozec, Y., Comeau, S., Conan, P., Coppola, L., Cuet, P., Ferreira, E., Gattuso, J.-P., Gazeau, F., Goyet, C., Grossteffan, E., Lansard, B., Lefèvre, D., Lefèvre, N., Leseurre, C., Petton, S., Pujo-Pay, M., Rabouille, C., Reverdin, G., Ridame, C., Rimmelin-Maury, P., Ternon, J.-F., Touratier, F., Tribollet, A., Wagener, T., and Wimart-Rousseau, C.: An updated synthesis of ocean total alkalinity and dissolved inorganic carbon measurements from 1993 to 2023: the SNAPO-CO_2-v2 dataset, Earth Syst. Sci. Data, 17, 1075–1100, https://doi.org/10.5194/essd-17-1075-2025, 2025.

Naegler, T., Ciais, P., Rodgers, K., and Levin, I.: Excess radiocarbon constraints on air-sea gas exchange and the uptake of CO_2 by the oceans, Geophysical Research Letters, 33, 2005GL025408, https://doi.org/10.1029/2005GL025408, 2006.

~~Nickford, S., Palter, J. B., Donohue, K., Fassbender, A. J., Gray, A. R., Long, J., Sutton, A. J., Bates, N. R., and Takeshita, Y.: Autonomous Wintertime Observations of Air-Sea Exchange in the Gulf Stream Reveal a Perfect Storm for Ocean CO_2 Uptake, Geophysical Research Letters, 49, e2021GL096805, https://doi.org/10.1029/2021GL096805, 2022.~~

Nickford, S., Palter, J. B., and Mu, L.: The Importance of Contemporaneous Wind and pCO_2 Measurements for Regional Air-Sea CO_2 Flux Estimates, JGR Oceans, 129, e2023JC020744, https://doi.org/10.1029/2023JC020744, 2024.

Nightingale, P. D., Malin, G., Law, C. S., Watson, A. J., Liss, P. S., Liddicoat, M. I., Boutin, J., and Upstill-Goddard, R. C.: In situ evaluation of air-sea gas exchange parameterizations using novel conservative and volatile tracers, Global Biogeochemical Cycles, 14, 373–387, https://doi.org/10.1029/1999GB900091, 2000.

Otero, P., Padin, X. A., Ruiz-Villarreal, M., García-García, L. M., Ríos, A. F., and Pérez, F. F.: Net sea–air CO_2 flux uncertainties in the Bay of Biscay based on the choice of wind speed products and gas transfer parameterizations, Biogeosciences, 10, 2993–3005, https://doi.org/10.5194/bg-10-2993-2013, 2013.

Ovchinnikov, I. M., Zats, V. I., Krivosheya, V. G., & Udodov, A. I.: Formation of deep Eastern Mediterranean waters in the Adriatic Sea. Oceanology, 25(6), 704-707, 1985.

Park, J., Stock, C. A., Yang, X., Dunne, J. P., Rosati, A., John, J., and Zhang, S.: Modeling Global Ocean Biogeochemistry With Physical Data Assimilation: A Pragmatic Solution to the Equatorial Instability, J Adv Model Earth Syst, 10, 891–906, https://doi.org/10.1002/2017MS001223, 2018.

~~Pecci, M., Sferlazzo, D., Anello, F., Becagli, S., Colella, S., Silvestri, L. D., Iorio, T. D., Meloni, D., Monteleone, F., Piacentino, S., Principato, E., and Sarra, A. D.: Large influence of the 2022-23 marine heatwave on the air-sea CO2 flux in the Central Mediterranean,https://doi.org/10.22541/essoar.173393985.55347710/v1, 11 December 2024.~~
Pecci, M., Sferlazzo, D., Anello, F., Becagli, S., Colella, S., De Silvestri, L., Di Iorio, T., Iaccarino, A., Meloni, D., Monteleone, F., Piacentino, S., Principato, E., and Di Sarra, A.: First Derivations of Air-Sea CO_2 Fluxes in the Central Mediterranean and Possible Impact of the 2022–2023 Marine Heatwave, JGR Oceans, 131, e2025JC023007, https://doi.org/10.1029/2025JC023007, 2026.

Peixoto, J.P. and Oort, A.H.: Physics of Climate. American Institute of Physics, New York. https://doi.org/10.1063/1.2809772, 1992.

Pérez, F. F., Becker, M., Goris, N., Gehlen, M., López-Mozos, M., Tjiputra, J., Olsen, A., Müller, J. D., Huertas, I. E., Chau, T. T. T., Cainzos, V., Velo, A., Benard, G., Hauck, J., Gruber, N., and Wanninkhof, R.: An Assessment of CO_2 Storage and Sea-Air Fluxes for the Atlantic Ocean and Mediterranean Sea Between 1985 and 2018, Global Biogeochemical Cycles, 38, e2023GB007862, https://doi.org/10.1029/2023GB007862, 2024.

Pirro, A., Martellucci, R., Gallo, A., Kubin, E., Mauri, E., Juza, M., Notarstefano, G., Pacciaroni, M., Bussani, A., and Menna, M.: Subsurface warming derived from Argo floats during the 2022 Mediterranean marine heat wave, State Planet, 4-osr8, 1–12, https://doi.org/10.5194/sp-4-osr8-18-2024, 2024.

Ravaioli, M., Bergami, C., Riminucci, F., Langone, L., Cardin, V., Di Sarra, A., Aracri, S., Bastianini, M., Bensi, M., Bergamasco, A., Bommarito, C., Borghini, M., Bortoluzzi, G., Bozzano, R., Cantoni, C., Chiggiato, J., Crisafi, E., D'Adamo, R., Durante, S., Fanara, C., Grilli, F., Lipizer, M., Marini, M., Miserocchi, S., Paschini, E., Penna, P., Pensieri, S., Pugnetti, A., Raicich, F., Schroeder, K., Siena, G., Specchiulli, A., Stanghellini, G., Vetrano, A., and Crise, A.: The RITMARE Italian Fixed-Point Observatory Network (IFON) for marine environmental monitoring: a case study, Journal of Operational Oceanography, 9, s202–s214, https://doi.org/10.1080/1755876X.2015.1114806, 2016.

Resplandy, L., Hogikyan, A., Müller, J. D., Najjar, R. G., Bange, H. W., Bianchi, D., Weber, T., Cai, W. -J., Doney, S. C., Fennel, K., Gehlen, M., Hauck, J., Lacroix, F., Landschützer, P., Le Quéré, C., Roobaert, A., Schwinger, J., Berthet, S., Bopp, L., Chau, T. T. T., Dai, M., Gruber, N., Ilyina, T., Kock, A., Manizza, M., Lachkar, Z., Laruelle, G. G., Liao, E., Lima, I. D., Nissen, C., Rödenbeck, C., Séférian, R., Toyama, K., Tsujino, H., and Regnier, P.: A Synthesis of Global Coastal Ocean Greenhouse Gas Fluxes, Global Biogeochemical Cycles, 38, e2023GB007803, https://doi.org/10.1029/2023GB007803, 2024.

Robinson, A. R., Leslie, W. G., Theocharis, A., and Lascaratos, A.: Mediterranean Sea Circulation, in: Encyclopedia of Ocean Sciences, Elsevier, 1689–1705, https://doi.org/10.1006/rwos.2001.0376, 2001.

Roether, W. and Schlitzer, R.: Eastern Mediterranean deep water renewal on the basis of chlorofluoromethane and tritium data, Dynamics of Atmospheres and Oceans, 15, 333–354, https://doi.org/10.1016/0377-0265(91)90025-B, 1991.

Roobaert, A., Resplandy, L., Laruelle, G. G., Liao, E., and Regnier, P.: Unraveling the Physical and Biological Controls of the Global Coastal CO_2 Sink, Global Biogeochemical Cycles, 38, e2023GB007799, https://doi.org/10.1029/2023GB007799, 2024.

Rubino, A., Gačić, M., Bensi, M., Kovačević, V., Malačič, V., Menna, M., Negretti, M. E., Sommeria, J., Zanchettin, D., Barreto, R. V., Ursella, L., Cardin, V., Civitarese, G., Orlić, M., Petelin, B., and Siena, G.: Experimental evidence of long-term oceanic circulation reversals without wind influence in the North Ionian Sea, Sci Rep, 10, 1905, https://doi.org/10.1038/s41598-020-57862-6, 2020.

Salon, S., Cossarini, G., Bolzon, G., Feudale, L., Lazzari, P., Teruzzi, A., Solidoro, C., and Crise, A.: Novel metrics based on Biogeochemical Argo data to improve the model uncertainty evaluation of the CMEMS Mediterranean marine ecosystem forecasts, Ocean Sci., 15, 997–1022, https://doi.org/10.5194/os-15-997-2019, 2019.

di Sarra, A., Di Iorio, T., Piacentino, S., and Sferlazzo, D.: ICOS ATC NRT CO2 growing time series from Lampedusa (8.0 m), 2025-04-01–2025-10-19, ICOS RI, [dataset], https://hdl.handle.net/11676/jZB47zujZMJcR_Hl5CtLEVHD, 2025.

Schlitzer, R., Roether, W., Oster, H., Junghans, H.-G., Hausmann, M., Johannsen, H., and Michelato, A.: Chlorofluoromethane and oxygen in the Eastern Mediterranean, Deep Sea Research Part A. Oceanographic Research Papers, 38, 1531–1551, https://doi.org/10.1016/0198-0149(91)90088-W, 1991.

Schroeder, K., and Chiggiato J. (Eds): Oceanography of the Mediterranean Sea: An introductory guide. Elsevier, 20232.

Sisma-Ventura, G., Bialik, O. M., Yam, R., Herut, B., and Silverman, J.: pCO2 variability in the surface waters of the ultra-oligotrophic Levantine Sea: Exploring the air–sea CO2 fluxes in a fast warming region, Marine Chemistry, 196, 13–23, https://doi.org/10.1016/j.marchem.2017.06.006, 2017.

Steinhoff, T., Gkritzalis, T., Jones, S., Macovei, V. A., Neill, C., Schuster, U., Akl, J., Arruda, R., Atamanchuk, D., Barry, M., Beaumont, L., Cantoni, C., Dickson, A., Fahning, J., Fought, J., Frangoulis, C., Gutiérrez-Loza, L., Hagan, C., Honkanen, M., Kielosto, S., Kinski, N., Körtzinger, A., Landschützer, P., Lauvset, S. K., Lawrence-Slavas, N., Li, Q., Luchetta, A., Malarde, D., Paulsen, M., Ritschel, M., Rutgersson, A., Sanders, R., Shitashima, K., Spaulding, R., Stamataki, N., Stenbäck, K., Sutton, A., Tatkiewicz, W., Telszewski, M., Theetaert, H., Tilbrook, B., and Wanninkhof, R.: The ICOS OTC *p* CO_2 instrument intercomparison, Limnology & Ocean Methods, lom3.10727, https://doi.org/10.1002/lom3.10727, 2025.

Takahashi, T., Sutherland, S. C., Sweeney, C., Poisson, A., Metzl, N., Tilbrook, B., Bates, N., Wanninkhof, R., Feely, R. A., Sabine, C., Olafsson, J., and Nojiri, Y.: Global sea–air CO2 flux based on climatological surface ocean pCO2, and seasonal biological and temperature effects, Deep Sea Research Part II: Topical Studies in Oceanography, 49, 1601–1622, https://doi.org/10.1016/S0967-0645(02)00003-6, 2002.

Tanhua, T., McCurdy, A., Fischer, A., Appeltans, W., Bax, N., Currie, K., DeYoung, B., Dunn, D., Heslop, E., Glover, L. K., Gunn, J., Hill, K., Ishii, M., Legler, D., Lindstrom, E., Miloslavich, P., Moltmann, T., Nolan, G., Palacz, A., Simmons, S., Sloyan, B., Smith, L. M., Smith, N., Telszewski, M., Visbeck, M., and Wilkin, J.: What We Have Learned From the Framework for Ocean Observing: Evolution of the Global Ocean Observing System, Front. Mar. Sci., 6, 471, https://doi.org/10.3389/fmars.2019.00471, 2019.

Touratier, F., Goyet, C., Houpert, L., De Madron, X. D., Lefèvre, D., Stabholz, M., and Guglielmi, V.: Role of deep convection on anthropogenic CO2 sequestration in the Gulf of Lions (northwestern Mediterranean Sea), Deep Sea Research Part I: Oceanographic Research Papers, 113, 33–48, https://doi.org/10.1016/j.dsr.2016.04.003, 2016.

Tsiaras, K., Frangoulis, C., and Stamataki, N.: Carbonate system variability in the Mediterranean Sea: a modelling study, Front. Mar. Sci., 11, 1347990, https://doi.org/10.3389/fmars.2024.1347990, 2024.

Turchetto, M., Boldrin, A., Langone, L., and Miserocchi, S.: Physical and biogeochemical processes controlling particle fluxes variability and carbon export in the Southern Adriatic, Continental Shelf Research, 44, 72–82, https://doi.org/10.1016/j.csr.2011.05.005, 2012a.

Turchetto, M., Boldrin, A., Langone, L., and Miserocchi, S.: Physical and biogeochemical processes controlling particle fluxes variability and carbon export in the Southern Adriatic, Continental Shelf Research, 44, 72–82, https://doi.org/10.1016/j.csr.2011.05.005, 2012b.

Ulses, C., Estournel, C., Marsaleix, P., Soetaert, K., Fourrier, M., Coppola, L., Lefèvre, D., Touratier, F., Goyet, C., Guglielmi, V., Kessouri, F., Testor, P., and Durrieu De Madron, X.: Seasonal dynamics and annual budget of dissolved inorganic carbon in the northwestern Mediterranean deep-convection region, Biogeosciences, 20, 4683–4710, https://doi.org/10.5194/bg-20-4683-2023, 2023.

Urbini, L., Ingrosso, G., Djakovac, T., Piacentino, S., and Giani, M.: Temporal and Spatial Variability of the CO2 System in a Riverine Influenced Area of the Mediterranean Sea, the Northern Adriatic, Front. Mar. Sci., 7, 679, https://doi.org/10.3389/fmars.2020.00679, 2020.

Vilibić, I. and Supić, N.: Dense water generation on a shelf: the case of the Adriatic Sea, Ocean Dynamics, 55, 403–415, https://doi.org/10.1007/s10236-005-0030-5, 2005.

Volpe, G., Colella, S., Brando, V. E., Forneris, V., La Padula, F., Di Cicco, A., Sammartino, M., Bracaglia, M., Artuso, F., and Santoleri, R.: Mediterranean ocean colour Level 3 operational multi-sensor processing, Ocean Sci., 15, 127–146, https://doi.org/10.5194/os-15-127-2019, 2019.

Wanninkhof, R. and McGillis, W. R.: A cubic relationship between air-sea CO_2 exchange and wind speed, Geophysical Research Letters, 26, 1889–1892, https://doi.org/10.1029/1999GL900363, 1999.

Wanninkhof, R.: Relationship between wind speed and gas exchange over the ocean revisited, Limnology & Ocean Methods, 12, 351–362, https://doi.org/10.4319/lom.2014.12.351, 2014.

Weiss, R. F.: Carbon dioxide in water and seawater: the solubility of a non-ideal gas, Marine Chemistry, 2, 203–215, https://doi.org/10.1016/0304-4203(74)90015-2, 1974.

Weiss, R. F. and Price, B. A.: Nitrous oxide solubility in water and seawater, Marine Chemistry, 8, 347–359, https://doi.org/10.1016/0304-4203(80)90024-9, 1980.

Zeebe, R. E. and Wolf-Gladrow, D.: CO2 in seawater: equilibrium, kinetics, isotopes, in: Elsevier Oceanography Series, vol. 65, edited by: Halpem, D., Elsevier B.V, Amsterdam, the Netherlands, 2001.